5-2011

Synthesis of 1-(5-methylhexyl)-2,3,8,9-tetrahydro-1H-naphtho[2,1-e]indol-6(7H)-one

Nicholas Lopez
College of William and Mary

Synthesis of 1-(5-methylhexyl)-2,3,8,9-tetrahydro-1*H*-naphtho[2,1-*e*]indol-6(7*H*)-one

A thesis submitted in partial fulfillment of the requirement
For the degree of Bachelors of Science in Chemistry from
The College of William and Mary

by

Nicholas Adam Lopez

Accepted for _____

_____

Dr. Christopher J. Abelt, Director

_____

Dr. Lisa M. Landino

_____

Professor Christine Westberg

Synthesis of 1-(5-methylhexyl)-2,3,8,9-tetrahydro-1*H*-naphtho[2,1-*e*]indol-6(7*H*)-one

A thesis submitted in partial fulfillment of the requirement
For the degree of Bachelors of Science in Chemistry from
The College of William and Mary

by

Nicholas Adam Lopez

Table of Contents

Acknowledgements

I would like to thank Professor Christopher J. Abelt for all of his support and guidance not only on this thesis but also in my four years at William and Mary. I would also like to thank everyone else who worked in Abelt lab for making this possible. I want to thank all of my friends and family for their support and love during this project. I could not have done this without their encouragement. I want to thank my Pastors and church leaders for their prayers and support. Finally, I want to thank God for His blessings and support.

"Trust in him at all times, you people; pour out your hearts to him, for God is our refuge." –Psalm 62:8

List of Figures

List of Schemes

Introduction

The goal of study was to explore the synthesis of 1-(5-methylhexyl)-2,3,8,9-tetrahydro-1*H*-naphtho[2,1-*e*]indol-6(7*H*)-one. The structure and ring designation of this molecule is shown in *Figure 1*.

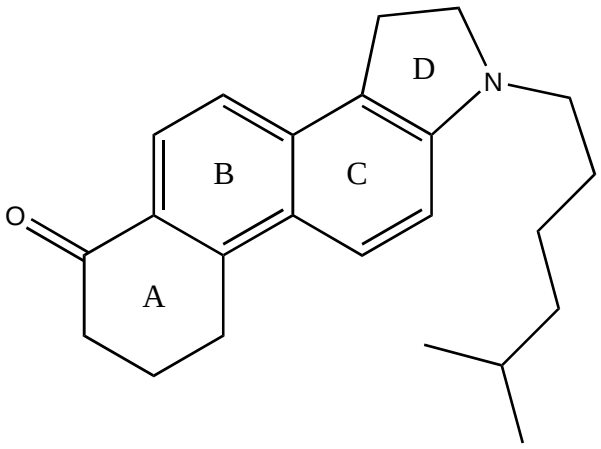

1-(5-methylhexyl)-2,3,8,9-tetrahydro-1*H*-naphtho[2,1-*e*]indol-6(7*H*)-one

Figure 1

This molecule is designed to act as a fluorescent model for cholesterol. It mimics cholesterol in terms of size, shape, and hydrophobic nature. This molecule gains its fluorescent character by having a fluorophore imbedded within its structure.

The fluorophore embedded within the model is essentially the fluorophore 1-(6-(dimethylamino)naphthalen-2-yl)propan-1-one, also called PRODAN, shown in *Figure 2*.

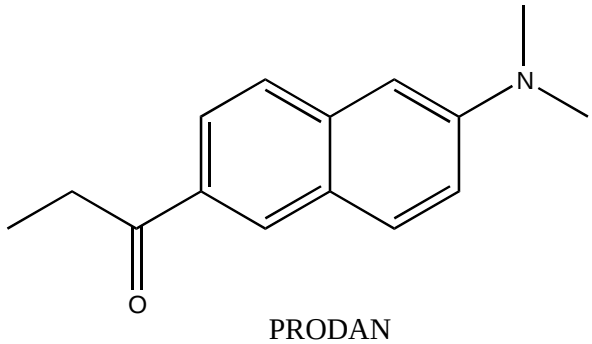

PRODAN

Figure 2

The two six-membered rings of PRODAN make up the B-ring and C-ring of the model. The amine is built into the five-membered D-ring, and the carbonyl functional group is attached to the A-ring of the model. A nine-step synthesis was explored in order to develop this model.

1-(5-methylhexyl)-2,3,8,9-tetrahydro-1*H*-naphtho[2,1-*e*]indol-6(7*H*)-one was designed to be used as a cholesterol model in order to explore the cholesterol binding sites of the protein human serum albumin (HSA). HSA has been shown to be involved in cholesterol transport.[i]

Background

Steroid hormones are terpene derivatives that are essential for cell signaling and homeostasis. The basic structure for all steroids is a four-fused ring system: three six-membered rings and one five-membered ring. The molecular precursor to all steroid hormones is cholesterol. The cholesterol structure as well as ring designation is shown in *Figure 3*.

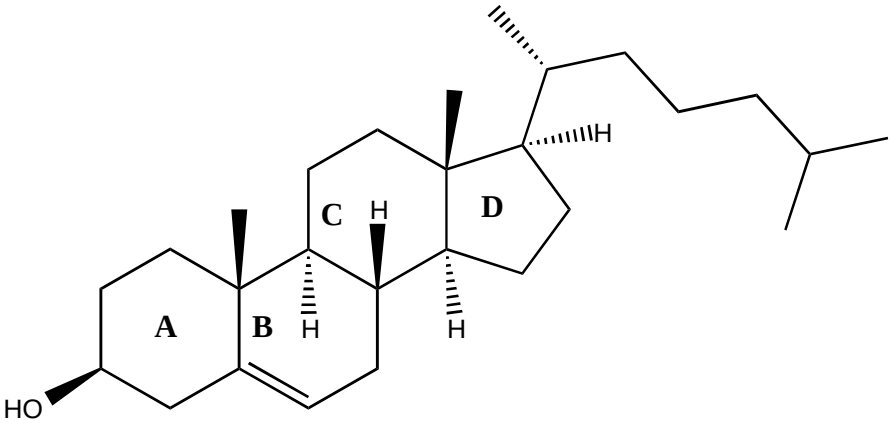

Figure 3

Cholesterol is located in all human cells tissue, but it is only slightly water-soluble. It must, therefore, be transported throughout the body by various lipoproteins. The two primary classes of lipoproteins that transport cholesterol are low-density lipoproteins (LDLs) and high-density lipoproteins (HDLs). LDLs are the primary transporters to cell tissue. High concentrations of LDLs can result in plaques that form on artery walls. HDLs transports scavenged cholesterol to the liver, where excess cholesterol can be disposed of. [ii] LDLs, HDLs, and cholesterol all play significant roles in heart disease.[iii]

HDLs and LDLs are not the only proteins that transport cholesterol. The protein Human Serum Albumin (HSA) has been shown to play a significant role in cholesterol trafficking.[iv] HSA is the most abundant protein in blood plasma with a concentration of around 5 g/100 mL.[v] It has been shown that HSA does not promote cholesterol efflux as well as other proteins but due to the fact that it is present in much higher concentration than other cholesterol transporters it plays a significant role in cholesterol transport.[vi]

HSA is a 66 kDa monomer of 585 amino acids. HSA contains a large amount of α-helical structures as well as 17 disulfide bonds and a single tryptophan residue. HSA is divided into three homologous helical domains named I, II, and III. Each of these domains is further subdivided into A and B subdomains.[vii]

The primary function of HSA is disputed but HSA is important in obtaining proper osmotic pressure and important in transport and regulatory processes. The substrates that bind to HSA include metals, fatty acids, amino acids, hormones, cholesterol, and many therapeutic drugs. [viii] HSA has been shown to contain eleven total binding sites for fatty acids. Up to seven of those binding sites can contain a long chain fatty acids simultaneously.[ix]

Because it plays such a vital role in fatty acid and cholesterol transport, HSA has been investigated in its role in heart disease. In fact, there is an association between the mortality rate and levels of HSA in serum. Low levels of HSA have been to correlated to high rates of mortality in coronary heart disease.[x, xi]

Despite the fact that HSA plays a major role in cholesterol efflux, there has been very little investigation into the relationship between HSA and cholesterol. Current research suggests that cholesterol binds to two separate sites. One site in subdomain IIA and the other site in subdomain IIIA.[xii] It has been shown that these two sites are the two primary binding sites for drugs.[xiii,xiv]

The goal of this research is to synthesize the fluorescent cholesterol analog that can be used to examine HSA-cholesterol binding properties. Because cholesterol binds so nonspecifically to HSA, the analog need only mimic cholesterol in terms of size, shape, hydrophobicity, and arrangement of polar groups.

It should be noted that, currently, there are fluorescent cholesterol models. There are two major problems with the current analogs. The first observed problem is that a large number of the current models have low quantum fluorescent yield. The other problem is that in order for the models to gain fluorescent character, they have significant structural differences from cholesterol.[xv]

Fluorescent cholesterol analogs have been used in specific protein studies as well as lipid membrane binding studies. Problems with the current models have arisen with both types of studies. In lipid membranes it has been shown that some models insert into the membrane upside down, or that the models do not interact with lipid rafts. In the case of protein binding sites, it has been shown that slight variations to the original cholesterol structures greatly reduce the binding affinity of the models. [xvi,xvii,xviii] HSA, a carrier protein, falls in-between these two

categories. The HSA-cholesterol binding sites possess a higher selectivity than lipid membranes but not the selectivity of specific protein binding sites. This is the reason why the model created in this study needed to only mimic cholesterol in terms of size, shape, hydrophobicity, and arrangement of polar groups. It is also important to note that HSA contains UV-absorbing chromophores, especially its tryptophan residue. Therefore a cholesterol analog must emit and absorb outside the range of tryptophan.

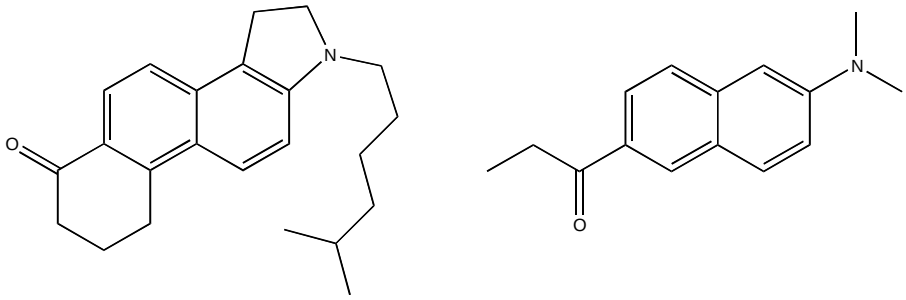

1-(5-methylhexyl)-2,3,8,9-tetrahydro-1*H*-naphtho[2,1-*e*]indol-6(7*H*)-one PRODAN

Figure 4

The model created in this study, 1-(5-methylhexyl)-2,3,8,9-tetrahydro-1*H*-naphtho[2,1-*e*]indol-6(7*H*)-one (Figure 4), is based on the molecular fluorophore PRODAN(1-(6-(dimethylamino)naphthalen-2-yl)propan-1-one). PRODAN has actually been used to examine the binding properties of HSA. PRODAN has been shown to bind to the drug binding site in the IIA and IIIA subdomains, the same sites cholesterol has been shown to bind to. Research suggests that interactions between PRODAN and HSA is largely due to hydrophobic and electrostatic interactions. [xix]

Fluorescence resonance energy transfer (FRET) studies have been conducted using PRODAN and HSA, specifically with Trp-214 and Cys-34. This

study showed that low concentrations of palmitic acid in the solution increased the fluorescence of PRODAN without effecting the tryptophan fluorescence but higher concentrations of palmitic acid had the opposite effect. This allowed for the mapping out of the binding locations of PRODAN and palmitic acid in relation to Trp-214 and Cys-34.[xx]

PRODAN was first prepared in 1979 by Weber and Ferris. It is a flurophore that is sensitive to the polarity of its environment. The fluorescent nature of PRODAN involves two groups, an electron donating alkylamino group and an electron accepting carbonyl. These two groups are attached to an aromatic naphthalene ring.[xxi]

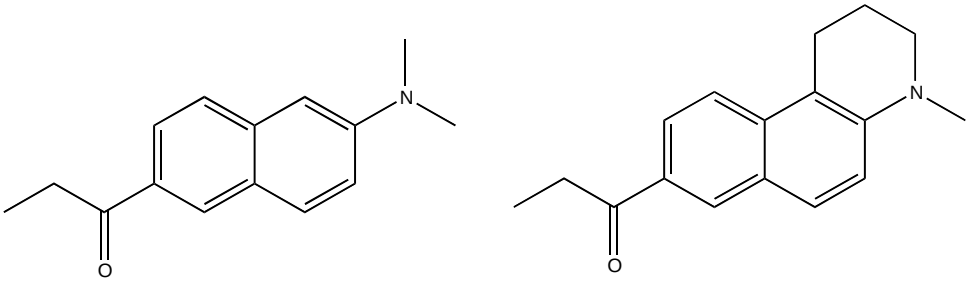

PRODAN Planar Model

Figure 5

Transfer of electron density from the electron donating group to accepting groups creates an excited state with significant fluorescent character . The Abelt lab has shown that if the amino group of PRODAN is constrained into a planar conformation (Figure 5) it possess nearly identical fluorescent characteristics to PRODAN. The twisted state, where the amino group is out of plane with the ring, however possesses nearly no fluorescent character.[xxii,xxiii] Within the model for this study the amino group is constrained in a five-membered ring in the planar conformation and will possess similar fluorescent characteristics to PRODAN.

Experimental

5-Bromonaphthalen-2-amine. 5-Bromonaphthalen-2-ol (7.23 g, 0.032 mol), $NaHSO_3$ (6.32 g, 0.061 mol), and NaOH (1.22 g, 0.031 mol) were placed in an autoclave followed by NH_4OH (60 mL). The autoclave was sealed and heated to 151℃ (~300 psi) overnight. The autoclave was allowed to cool to 60℃ and depressurized. The contents were extracted by rinsing with water and acetone. This mixture was poured into water (200 mL), and the mixture was stirred overnight to allow acetone to evaporate. The next day NaCl (25 g) was added to the mixture. The resulting precipitate was collected by suction filtration and then dissolved in CH_2Cl_2 (100 mL). HCl (50 mL, 10%) was added to the solution. A brown precipitate salt immediately forms and is collected through suction filtration. The precipitate is placed in aq. $NaHCO_3$ (300 mL, 2%) and stirred for 3 hours. The layers of the filtrate were separated, and the organic layer was concentrated *in vacuo* to obtain starting 5-bromonaphthalen-2-ol (3.46 g, 0.016 mol). The precipitate in the $NaHCO_3$ mixture is collected through suction filtration giving 5-bromonaphthalen-2-amine (3.05 g, 0.0137 mol, 81%, based on recovered starting material). ^{1}H NMR ($CDCl_3$) δ 8.03 (d, *J*= 8.8 Hz, 1H), 7.52 (d, *J*=8.2 Hz, 1 H), 7.49 (d, *J*=7.2 Hz, 1 H), 7.17 (t, *J*=7.0 Hz, 1 H), 7.00 (d, *J*=8.43 Hz, 1H), 6.93 (s, 1H); ^{13}C NMR ($CDCl_3$) δ 145.08, 136.43, 128.77, 126.93, 126.61, 126.53, 126.03, 123.03, 119.60, 108.89.

***N*-(5-Bromonaphthalen-2-yl)methanesulfonamide.** Pyridine (4.7 mL) is added with stirring to a solution of 5-bromonapthalen-2-amine (4.21 g, 0.019 mol) in

CH_2Cl_2 (60 mL) cooled to 0℃. Next, a solution of methanesulfonyl chloride (3.27 g, 0.029 mol) in CH_2Cl_2 (10 mL) is added dropwise. The mixture is stirred at 0℃ for 1 hour, then stirred at room temperature for 1 hour. The mixture is poured into saturated aq. $NaHCO_3$, and the layers are stirred together rapidly for 15 minutes. The product is extracted with CH_2Cl_2 (3x 50 mL). The combined organic layers are washed with 10% HCL (4x 50 mL), dried over Na_2SO_4, and concentrated *in vacuo*. The resulting solid was recrystallized in MeOH/H_2O. Finally, *N*-(5-bromonaphthalen-2-yl)methanesulfonamide was dried under high vacuum at 100℃ before the next step. (4.52 g, 0.015 mol, 79%). ^{1}H NMR ($CDCl_3$) δ 8.16 (d, *J*=9.1 Hz, 1H), 7.75 (d, *J*=7.75 Hz, 1H), 7.68 (d, *J*=7.3 Hz, 1H), 7.53 (d, J=8.7 Hz, 1H), 7.38 (s, 1H), 7.30 (t, *J*=7.9 Hz, 1H), 3.01 (s, 3H); ^{13}C NMR ($CDCl_3$) δ 136.83, 135.31, 129.14, 129.06, 128.79, 127.61, 127.18, 122.61, 121.69, 116.07, 39.32.

_N_-(5-Bromonaphthalen-2-yl)-_N_-(2,2-diethoxyethyl)methanesulfonamide. Potassium carbonate (2.35 g, 0.017 mol) is added to a solution of *N*-(6-bromonaphthalen-2-yl)methanesulfonamide (2.50g, 0.00833 mol) is added to DMF (10 mL) under Ar followed by addition of K_2CO_3 (1 g, 0.00725 mol). 2-bromo-1,1-diethoxyethane (3 mL, 0.0116 mol) is added. The reaction mixture is heated overnight at 110℃ with stirring. The reaction is monitored by TLC. Another portion of 2-bromo-1,1-diethoxyethane (1 mL, 0.00387 mol) is added, and heating and stirring is continued overnight. A further portion of 2-bromo-1,1-diethoxyethane (1 mL, 0.00387 mol) is added, and heating and stirring is

continued overnight. Additional K_2CO_3 (0.42 g, 0.00305 mol) and 2-bromo-1,1-diethoxyethane (1 mL, 0.00387 mol) are added. When TLC analysis shows that the reaction is complete, the reaction is allowed to cool. The inorganic solids are removed by suction filtration, and the solid is washed with a small amount of CH_2Cl_2. The volatile solvent is removed *in vacuo*, and the higher boiling materials are removed under high vacuum (0.1 Torr, up to 145°C) distillation. *N*-(5-Bromonaphthalen-2-yl)-*N*-(2,2-diethoxyethyl) methanesulfonamide is collected with some solvent still present on the solid (3.91 g, 0.0940, 112%). ^{1}H NMR ($CDCl_3$) δ 8.27 (d, *J*=9.0 Hz, 1H), 7.86 (s, 1H) 7.80 (d, *J*=6.9 Hz, 1H), 7.79(d, *J*=7.95 Hz, 1H), 7.57 (d *J*=8.39, Hz 1H), 7.36 (t, *J*=7.61 Hz, 1H), 4.63 (t, *J*=5.4 Hz, 1H) 3.88 (d, *J*=5.26 Hz, 2H), 3.64(q, *J*=7.71 Hz, 2H), 3.49 (q, *J*=7.6 Hz, 2H), 3.01(s, 3H), 1.13 (t, *J*=6.91 Hz, 6); ^{13}C NMR ($CDCl_3$) δ 138.73, 134.91, 131,31, 130,89, 129,05, 128.20, 127.67, 127.64, 127.34, 122.83, 101.24, 62.86, 53.55, 38.66, 15.45

6-Bromo-3-(methylsulfonyl)-3*H*-benzo[*e*]indole. The *N*-(5-Bromonaphthalen-2-yl)-*N*-(2,2-diethoxyethyl)methanesulfonamide residue (~3.91 g, ~0.0940 mol) is dissolved in CH_2Cl_2 (20 mL) and boron trifluoride etherate (1.5 mL, 0.0122 mol) is added. The reaction is stirred at room temperature overnight. The reaction is monitored by TLC. The following day two more portions of boron trifluoride etherate (0.5 mL, 0.00407 mol) is added, and the reaction is stirred at room temperature overnight. A final portion of boron trifluoride etherate (0.5 mL, 0.00407 mol) is added. The reaction mixture is poured slowly into saturated aq.

NaHCO3 (200 mL) with vigorous stirring. Once the bubbling has stopped, CH_2Cl_2 (100 mL) is added to the mixture, and the layers are separated. The aqueous layer is extracted with CH_2Cl_2 (2x 50 mL). The organic layers are washed with H_2O (2x 50 mL), dried over $CaCl_2$, and concentrated *in vacuo*. 6-Bromo-3-(methylsulfonyl)-3*H*-benzo[*e*]indole was collected (2.66 g, 0.00821 mol, 87%). ^{1}H NMR ($CDCl_3$) δ 8.18 (m, 3 H), 7.81 (d, *J*=7.1 Hz, 1 H), 7.60 (d, *J*=2.9 Hz, 1H), 7.43 (t, *J*=7.9 Hz, 1H), 7.22 (d, *J*=2.86 Hz, 1 H), 3.17 (s, 3H); ^{13}C NMR ($CDCl_3$) δ 129.55, 129.12, 128.99, 127.35, 127.29, 126.74, 125.75, 123,78, 123.32, 114, 32, 107.38, 41.90

6-Bromo-3*H*-benzo[*e*]indole. The 6-Bromo-3-(methylsulfonyl)-3*H*-benzo[*e*]indole (2.66 g, 0.00821 mol) residue is taken up in 5% methanolic KOH (150 mL), and the reaction is refluxed overnight. The reaction is allowed to cool, and the mixture is poured into H_2O (300 mL). The methanol is allowed to evaporate overnight. The resulting solid is collected via suction filtration, washed with water and air-dried. The filtrate is acidified with acetic acid (50 mL), NaCl is added, and the resulting solid is collected through suction filtration, washed with water, and air-dried giving N-(5-bromonaphthalen-2-yl)methanesulfonamide (140 mg, 0.466 mmol). The first solid is purified by high vacuum (0.1 Torr, T ~ 200 °C) sublimation giving 6-bromo-3H-benzo[e]indole (0.78g, 0.00317 mol, 28 %) From *N*-(5-bromonaphthalen-2-yl)methanesulfonamide (40% over 3 steps). ^{1}H NMR ($CDCl_3$) δ 8.21 (d, *J*=7.9 Hz, 1H), 8.03 (d, *J*=9.14 Hz, 1H), 7.71 (d, *J*=7.66 Hz, 1H), 7.61 (d, *J*=9.1 Hz, 1H), 7.37 (t, *J*=7.46 Hz, 1H), 7.31 (s, 1H), 7.08 (s,

1H); ^{13}C NMR ($CDCl_3$) δ 129.73, 127.86, 127.81, 126.35, 123.76, 123.26, 123.23, 123.17, 123.10, 122.12, 114.26, 102.39.

6-bromo-3-(5-methylhexyl)-3*H*-benzo[*e*]indole. Sodium hydride (150 mg, 0.00625 mol, 60% in oil) is added in one portion to a solution of 6-bromo-3H-benzo[e]indole (0.78 g, 0.00317 mol) in DMF (15 mL). After the reaction is complete, 5-methylhexyl methanesulfonate (1.00 g, 0.00309 mol) is added in one portion. The reaction is stirred under N_2 for several hours. Additional sodium hydride (70 mg, 0.0030mol) is added and stirred for 15 minutes. Then additional 5-methylhexyl methanesulfonate (240 mg, 1.24 mmol) is added and stirred under N_2 overnight. The next day TLC analysis show that the reaction is complete. The next day the reaction mixture is diluted with hexanes (45 mL) and CH_2Cl_2 (15 mL). The aqueous layer is additionally extracted with hexanes (20 mL) and CH_2Cl_2 (10 mL). The combined organic layer is washed with water (3 x 60 mL), then dried over $CaCl_2$, and conc. *in vacuo*. The excess 5-methylhexyl methanesulfonate is removed by vacuum distillation (0.1 Torr, up to 190°C) leaving 6-bromo-3-(5-methylhexyl)-3H-benzo[e]indole (~1.04 g, 0.00302 mol, 95.3%) which is used without further purification. ^{1}H NMR ($CDCl_3$) δ 8.22 (d, *J*=7.99 Hz, 1 H), 8.04 (d, *J*= 9.15 Hz, 1H), 7.71 (d, *J*= 7.16 Hz, 1H), 7.60 (d, *J*= 9.52 Hz, 1H), 7.37 (t, *J*=7.73 Hz, 1H), 7.21 (d, *J*=2.38 Hz, 1H), 7.03 (d, *J*=2.67 Hz, 1H), 4.22 (t, *J*=7.0 Hz, 2H), 1.86 (q, *J*=7.05 Hz, 2H), 1.52(m, *J*=6.6 Hz, 1H), 1.31(p, *J*=7.8 Hz, 2H), 1.22 (p, *J*=7.1 Hz, 2H), 0.87(d, *J*=6.3 Hz, 6H); (CDCl3) δ

132.92, 129.96, 127.56, 126.87, 126.22, 123.77, 123.73, 122.95, 121.38, 113.01, 112.77, 100.67, 46.98, 38.70, 31.24, 28.11, 24.95, 22.81.

6-Bromo-3-(5-methylhexyl)-2,3-dihydro-1*H*-benzo[*e*]indole. 6-bromo-3-(5-methylhexyl)-3*H*-benzo[*e*]indole (1.04 g, 3.02 mmol) is combined with AcOH (25 mL). $NaBH_3CN$ (2.0 g, 0.0317 mol) is added slowly to mixture, and the reaction is left to stir overnight under N_2. The next day additional $NaBH_3CN$ (1 g, 0.0159 mol) is added, and the reaction is stirred for several hours. The product mixture is added dropwise to aq. sodium bicarbonate (300 mL, 40 g), and the mixture is stirred for 1 hr. The product was extracted with CH_2Cl_2 (3x 100 mL), washed with H_2O (2x 100 mL), concentrated *in vacuo*, and purified by high vacuum (0.1 Torr, up to 145 °C) distillation to give 6-bromo-3-(5-methylhexyl)-2,3-dihydro-1*H*-benzo[*e*]indole (900 mg, 2.60 mol, 86%). ^{1}H NMR ($CDCl_3$) δ 8.04 (d, *J*=8.8 Hz, 1H), 7.46(m, *J*=9.0 Hz, 2H), 7.19(t, *J*=7.9 Hz, 1H), 6.98(d, J=9.1 Hz, 1H), 3.55(t, *J*=8.5 Hz, 2H), 3.24(t, *J*=8.7 Hz, 2H), 3.17(t, *J*=7.3 Hz, 2H), 1.59(m, 3H), 1.42(p, *J*=7.7 Hz, 2H), 1.26(p, *J*=7.1 Hz, 2H), 0.92(d, *J*=6.8 Hz, 6H); ^{13}C NMR ($CDCl_3$) δ 151.46, 132.32, 127.92, 126.74, 126.21, 125.46, 123.93, 122.21, 121.38, 111.87, 53.72, 49.76, 39.09, 28.24, 27.93, 27.35, 25.27, 22.91.

Ethyl 4-(3-(5-methylhexyl)-2,3-dihydro-1*H*-benzo[*e*]indol-6-yl)butanoate. $NiCl_2(Pd_3)_2$ (176 mg, 2.69) is added to 6-bromo-3-(5-methylhexyl)-2,3-dihydro-1*H*-benzo[*e*]indole (900 mg, 2.62) in DMAC (7 mL) under N_2. The reaction is

stirred for 15 minutes until all the $NiCl_2(Pd_3)_2$ dissolves. 4-Ethoxy-4-oxobutylzinc bromide (8.8 mL, 0.5 M solution in THF, 4.4 mmol) is added to the mixture. Stirring continued for several hours. Additional $NiCl_2(Pd_3)_2$ (90 mg, 0.138 mmol) is added. After 15 minutes additional 4-ethoxy-4-oxobutylzinc bromide (5 mL, 0.5 M solution in THF, 2.5 mol) is added to the mixture. The reaction is monitored by TLC. Stirring continues overnight. The following day additional $NiCl_2(Pd_3)_2$ (90 mg, 0.138 mol) is added. After 15 minutes additional 4-ethoxy-4-oxobutylzinc bromide (5 mL, , 0.5 M solution in THF, 2.5 mmol) is added to the mixture. Stirring continues overnight. The following day the mixture is poured into water (300 mL) and stirred for 1 hour. Salt is added to the mixture and then the precipitated solid is collected with suction filtration. The solid is washed with water, air dried and ethyl 4-(3-(5-methylhexyl)-2,3-dihydro-1*H*-benzo[*e*]indol-6-yl)butanoate (1.33 g, 3.49 mol, >100%) is collected. ^{1}H NMR ($CDCl_3$) δ 7.87 (d, *J*=8.7 Hz, 1H), 7.46 (m, 1H), 7.01 (d, *J*=6.3 Hz, 1H), 6.95 (d, *J*=6.3 Hz, 1H), 4.12 (q, *J*=6.9 Hz, 2H), 3.5 (t, *J*=8.3 Hz, 2H), 3.24 (t, *J*=8.4 Hz, 2), 3.15(t, *J*=7.1 Hz, 2H), 3.04(t, *J*=7.6 Hz, 2H), 2.29 (t, *J*=7.3 Hz, 2H), 2.06 (p, *J*=7.3 Hz, 2H), 1.58(m, 2H), 1.40(m, 1H), 1.35(m, 2H), 1.25(t, *J*=6.4 Hz, 3H), 0.89(d, *J*=6.4 Hz, 6H); ^{13}C NMR ($CDCl_3$) δ

1-(5-methylhexyl)-2,3,8,9-tetrahydro-1*H*-naphtho[2,1-*e*]indol-6(7*H*)-one. Ethyl 4-(3-(5-methylhexyl)-2,3-dihydro-1*H*-benzo[*e*]indol-6-yl)butanoate(1.33 g, 3.49 mmol) is covered in polyphosphoric acid, heated to 110°C, and stirred overnight. The following day the mixture is poured into water (400 mL) and

stirred for several hours. The precipitated solid is collected with suction filtration and air dried. The solid was purified by vacuum (0.1 Torr, T ~ 200 °C) sublimation giving 1-(5-methylhexyl)-2,3,8,9-tetrahydro-1*H*-naphtho[2,1-*e*]indol-6(7*H*)-one (420 mg, 1.26 mol, 36%) (48% over two steps). ^{1}H NMR ($CDCl_3$) δ 8.01 (d, *J*=8.5 Hz, 1H), 7.93 (d, *J*=8.9 Hz, 1H), 7.40 (d, *J*=8.3 Hz, 1H), 6.93(d, *J*=8.9 Hz, 1H), 3.61(t, *J*=8.6 Hz, 2H), 3.27(m, 4), 3.21(t, *J*=7.0 Hz, 2H), 2.68(t, *J*=5.9 Hz, 2H), 2.24(t, *J*=5.6 Hz, 2H), 1.61(q, *J*=7.4 Hz, 2H), 1.54 (m, 1H), 1.39 (p, *J*=5.9 Hz, 2H), 1.24 (p, *J*=8.0 Hz, 2H), 0.89 (d, *J*=6.1 Hz, 6H).

Results and Discussion

The 1-(5-methylhexyl)-2,3,8,9-tetrahydro-1*H*-naphtho[2,1-*e*]indol-6(7*H*)-one cholesterol model has five main molecular components: the A-ring, B-ring, C-ring, D-ring, and alkyl chain tail. The B- and C-rings are the two six membered rings in the naphthalene of the starting compound 5-bromonaphthalen-2-ol. Previous work had allowed for successful synthesis of the A-ring using a Negishi coupling and Lewis acid ring closure. The alkyl chain was provided by the commercially available alcohol. Three separate pathways were explored for the synthesis of the D-ring. (*Figure 6*)

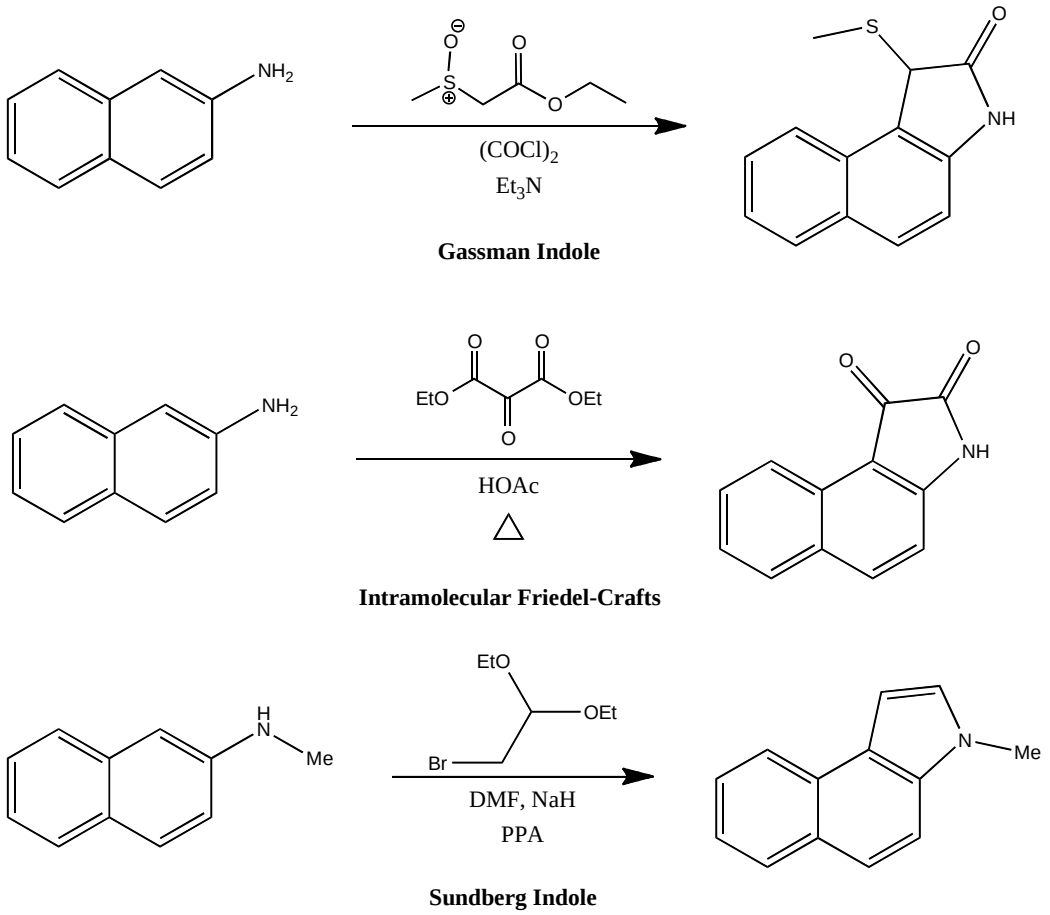

Figure 6

Each of the pathways was tested on the model compound, naphthalen-2-amine. The Gassman indole synthesis employed the use of a sulfoxide and a [2,3]-sigmatropic rearrangment as a means of cyclization. The problem with this synthesis arose in the difficulty of the removal in the thiol. With the intramolecular Friedel-Crafts synthesis, the multiple reduction steps lead to low yields. The Sundberg indole synthesis was selected for the D-ring synthesis due to the highest yields and ease of reactions.

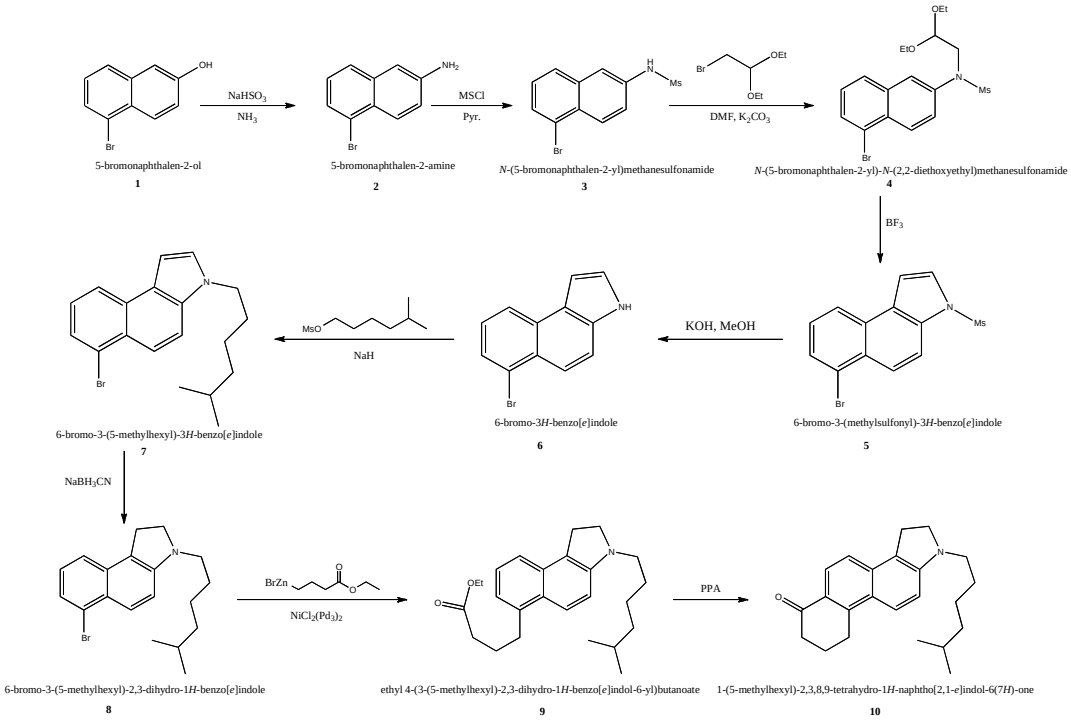

Scheme 1

The final target, **Compound 10**, 1-(5-methylhexyl)-2,3,8,9-tetrahydro-1*H*-naphtho[2,1-*e*]indol-6(7*H*)-one, was synthesized over a ten-step process starting from **1**, 5-bromonaphthalen-2-ol (*Scheme 1*). As mentioned above the B- and C-rings were imbedded in the 5-bromonaphthalen-2-ol starting material and the D-ring was added to the naphthalene base using the Sundberg indole synthesis. The

alkyl chain was attached to the amine within the D-ring, and finally the A-ring was added using a Negishi Coupling reaction followed by Lewis acid cyclization.

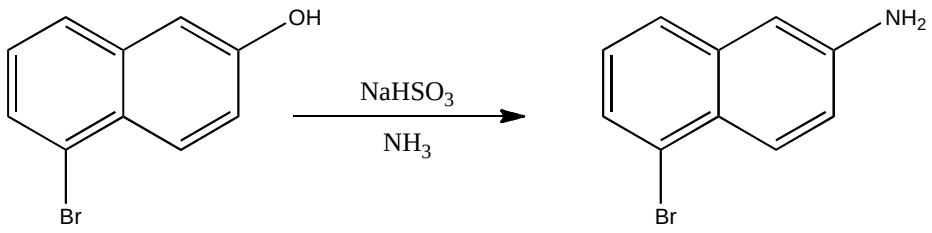

5-bromonaphthalen-2-ol **1**

5-bromonaphthalen-2-amine **2**

Scheme 2

Compound 2 was prepared in 81% yield (*Scheme 2*). Reactant **1** was recovered, and the yield was based on this recovery. Reactant **1** was prepared by Abelt lab. The Bucherer reaction was performed on **1** to give **2.** This reaction was performed in autoclave at >150 °C and ~300 psi overnight. Initially, the autoclave would not hold pressure, and the reaction would proceed with very low yields. Cleaning the autoclave and double-wrapping the O-ring with Teflon tape solved this problem. ^{1}H and ^{13}C confirmed the transformation. The appropriate aromatic peaks appeared (7-8 pmm) as well as ten carbon peaks. The same number of peaks with the same patterns as **1** appeared. However, there were chemical shift changes consistent with the substitution of a greater resonance-electron donating group.

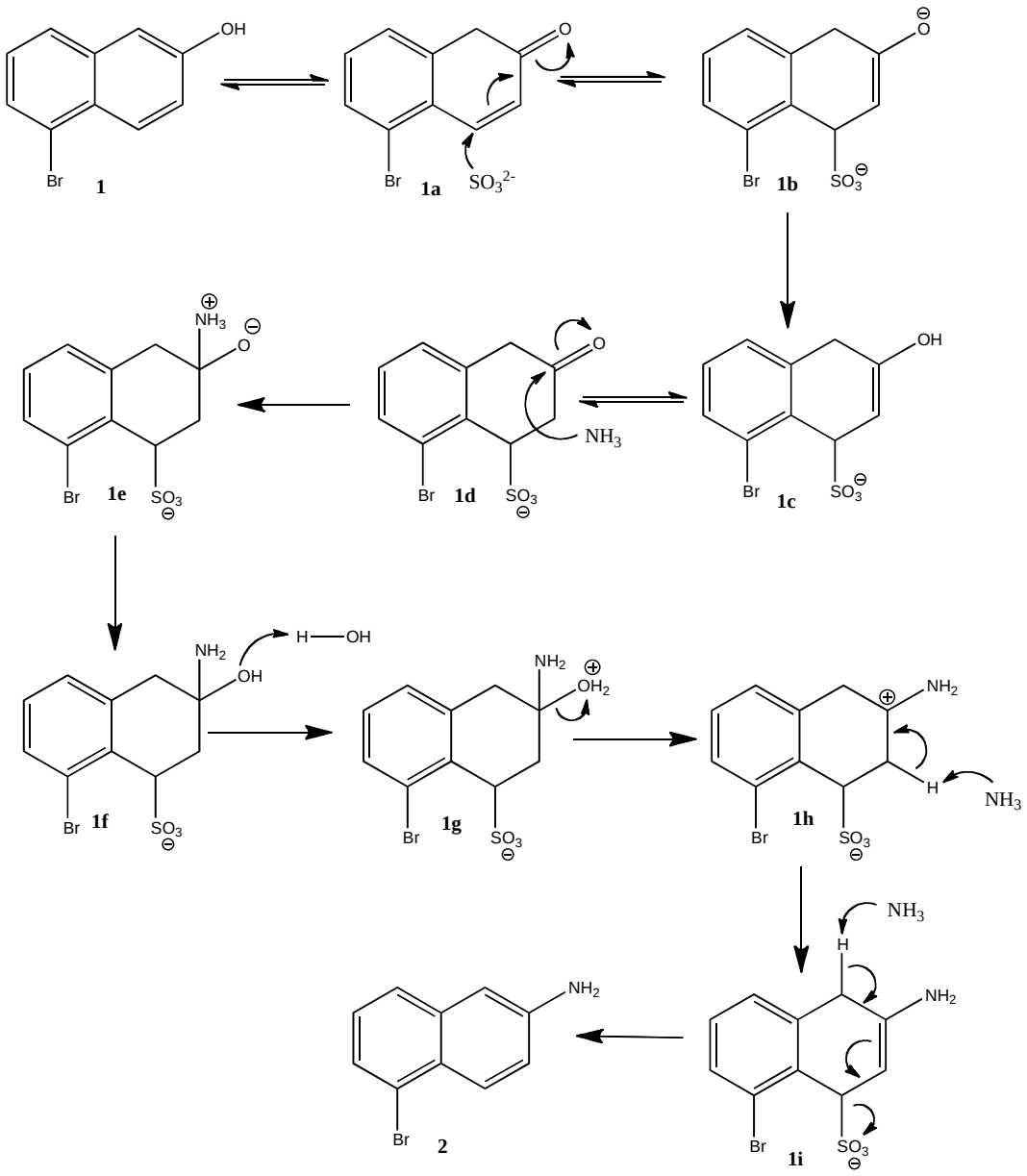

Figure 7

The mechanism for the Bucherer reaction is of interest and is illustrated in *Figure 7.* First the sulfite adds to the keto resonance form **1a** at the beta position to the carbonyl. After protonation, the alcohol **1c** is formed. After tautomerization, the carbonyl on the resonance form **1d** suffers nucleophilic attack by ammonia**.** The alcohol in **1f** takes up a second hydrogen becoming a

good leaving group. The hydronium ion leaves from **1g** and the alpha carbon is deprotonated in **1h** reforming one of the pi bonds. It is also possible that at these temperatures for the hydroxide to leave without protonation. Finally, aromaticity is restored when the sulfite leaves **1i** resulting in product **2**.

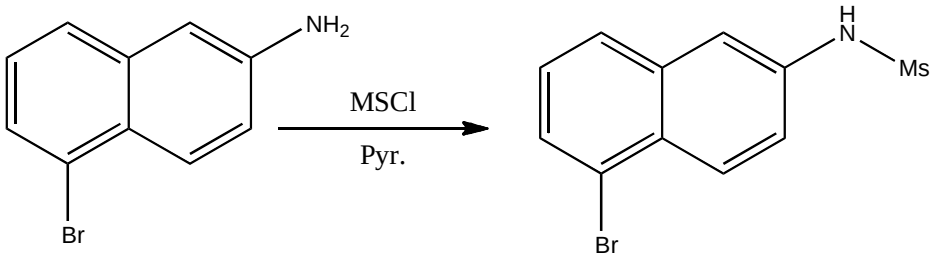

5-bromonaphthalen-2-amine

2

N-(5-bromonaphthalen-2-yl)methanesulfonamide

3

Scheme 3

Compound 3 was synthesized with a 79% yield. (*Scheme 3*) This reaction was performed in CH_2Cl_2 under $CaCl_2$. The mesylate functional group was successfully added to the amine of compound **2** through an addition-elimination mechanism. Compound **3** was purified by recrystalization.

The identity of **Compound 3** was confirmed by ^{1}H and ^{13}C NMR. The ^{1}H spectra had the appropriate ^{1}H aromatic peaks (7-8 ppm) and the strong singlet around 3 ppm indicating the methyl on the mesylate. The ^{13}C spectra had the expected 11 carbon peaks. The next several steps were performed without purification after each step. Purification was accomplished with **Compound 6**.

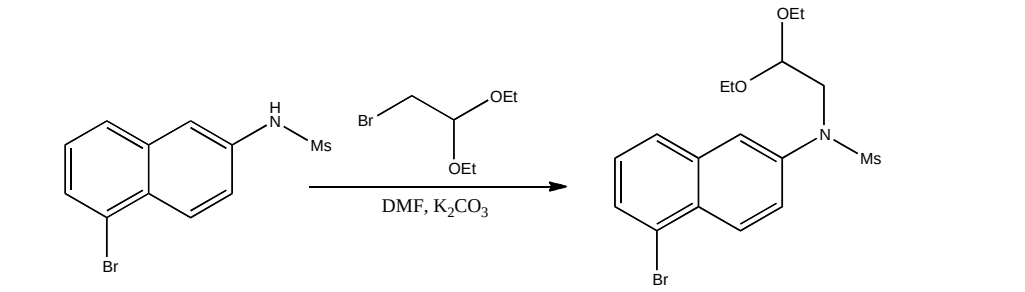

N-(5-bromonaphthalen-2-yl)methanesulfonamide
3

N-(5-bromonaphthalen-2-yl)-*N*-(2,2-diethoxyethyl)methanesulfonamide
4

Scheme 4

Compound 4 was prepared in over 100% yield (*Scheme 4*). This apparent yield is due to the fact that not all of the DMF solvent could be removed from the sample. Initially, quantitative amounts of NaH were used instead of K_2CO_3, but K_2CO_3 proved to give higher yields and was easier to use as additional portions of NaH had to be added with each addition of acetal. It is also imperative that pure DMF is used.

This reaction was monitored by TLC analysis using 75% hexanes/ 25% EtOAc. The slower eluting reactant, would become less intense through out the reaction, and the faster eluting product, would become more intense. Usually two to four additional amounts of acetal were required for the reaction to go to completion. This reaction proceeds by an S_N2 mechanism where, after it has been deprotonated, the nitrogen's lone pair attacks the carbon bearing the bromine on the acetal.

The identity of **Compound 4** was confirmed by ^1H and ^{13}C NMR. The appropriate ^1H aromatic peaks were observed (7-8 ppm) as well as the mesylate peak around 3 ppm. The appropriate ethyl peaks were observed downshifted due to the oxygen (3-4 ppm). A distinctive doublet-triplet pattern was observed for the

added two-carbon chain. The expected 15 carbon peaks were observed in the ^{13}C NMR.

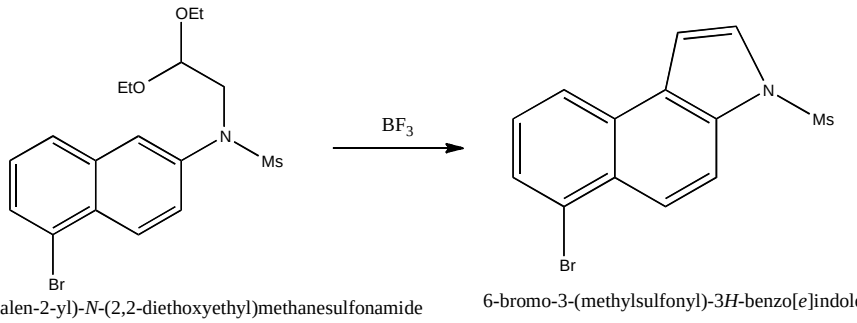

N-(5-bromonaphthalen-2-yl)-*N*-(2,2-diethoxyethyl)methanesulfonamide
4

6-bromo-3-(methylsulfonyl)-3*H*-benzo[*e*]indole
5

Scheme 5

Compound 5 was produced at 87% yield (*Scheme 5*). The Lewis acid, boron trifluoride, was used for the ring closure. Initially, polyphosphoric acid (PPA) was used, but boron triflouride proved to be easier to use as PPA is highly viscous.

This reaction was monitored by TLC analysis. A solution of 4% EtOAc/ 96% hexanes was used as the mobile phase. It would generally take 3 additional additions of BF_3 for the reactant spot to fully disappear.

The identity of **Compound 5** was confirmed by ^{1}H and ^{13}C NMR. The appropriate aromatic peaks appeared (7-8 ppm) as well as the mesylate peak around 3. The confirmation of ring closure is the indole peaks at 7.2 ppm (J=2.9 Hz) and at 7.6 ppm (J=2.9 Hz). The small J values are due to the hydrogen being a member of a 5-membered ring as well as the hydrogen's proximity to electronegative nitrogen. This small J value is a good indicator of the presence of the indole. The expected 13 carbon peaks were observed in the ^{13}C NMR.

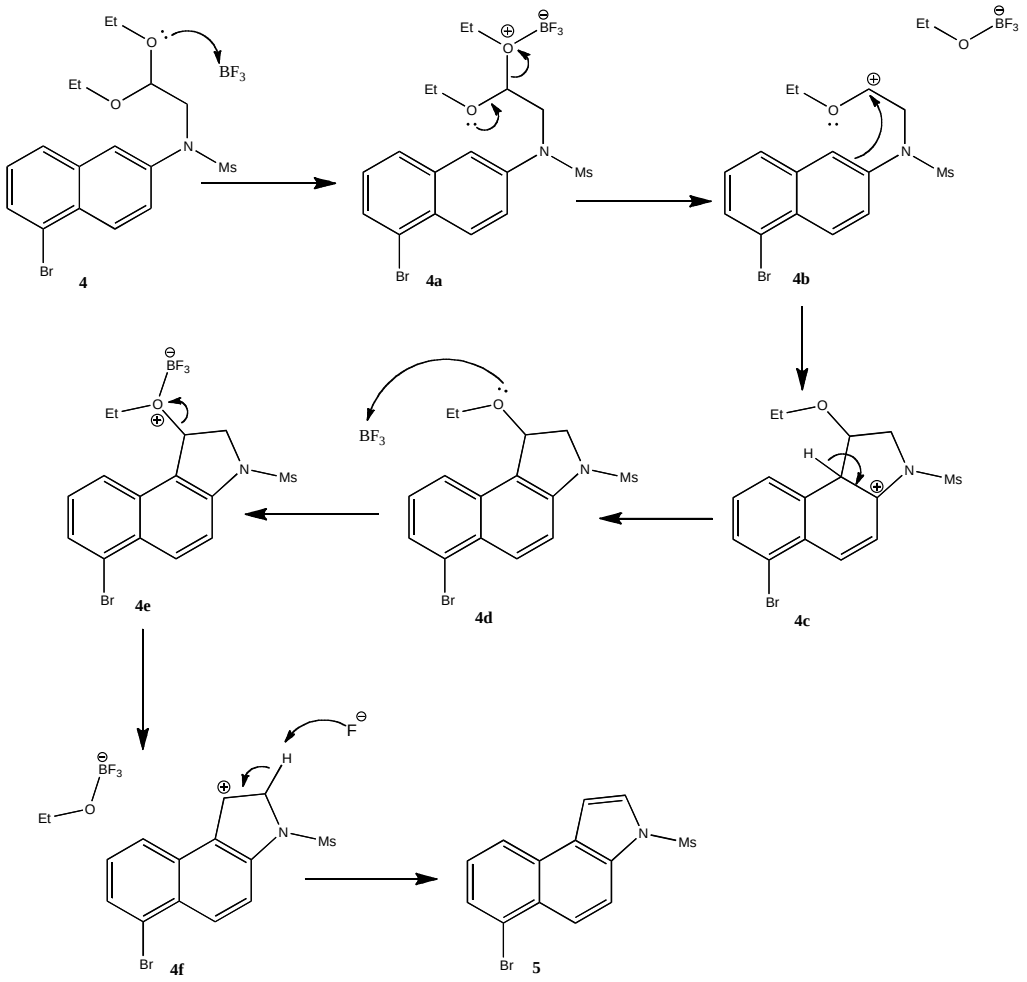

Figure 8

The mechanism for D-ring closure is worth noting and is shown in *Figure 8*. One of the oxygens on **4** acts as a nucleophile and bonds with BF_3. The formed ethoxytrifluoroborate leaves in **4a** and the electrons on the other oxygen help stabilize the cation that is formed. Then the pi electrons in the aromatic ring of **4b** nucleophillically attack the cation forming the 5-membered ring. After aromaticity is restored in **4d**, the remaining oxygen also bonds with BF_3 and

leaves as ethoxytrifluoroborate in **4e**. After further deprotationation, the indole that forms, **Compound 5**, is a stabilized heteroaromatic system.

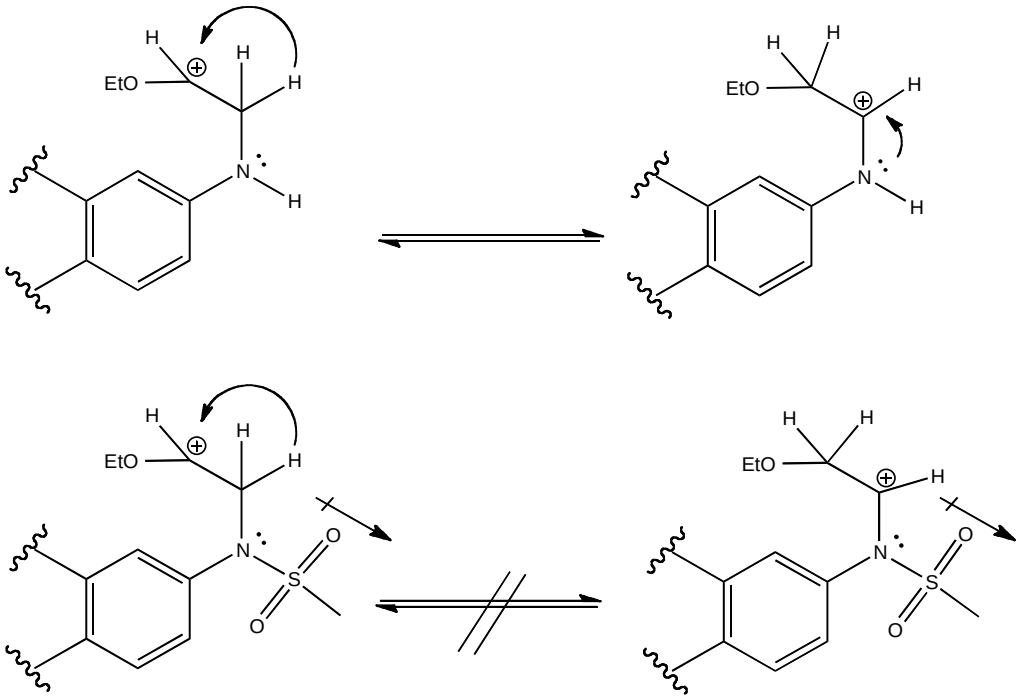

Figure 9

It is essential that the mesylate functional group is present, and *Figure 9* illustrates this fact. Without this mesylate group the cation in the intermediate could rearrange as the electrons on the nitrogen could help stabilize the positive charge. This does not occur in the presence of the mesylate because those electrons are delocalized to the mesylate and do not contribute to the cation stability. The likelihood of rearrangment is very small. This allows for the pi-electrons of the naphthalene to form the 5-membered ring.

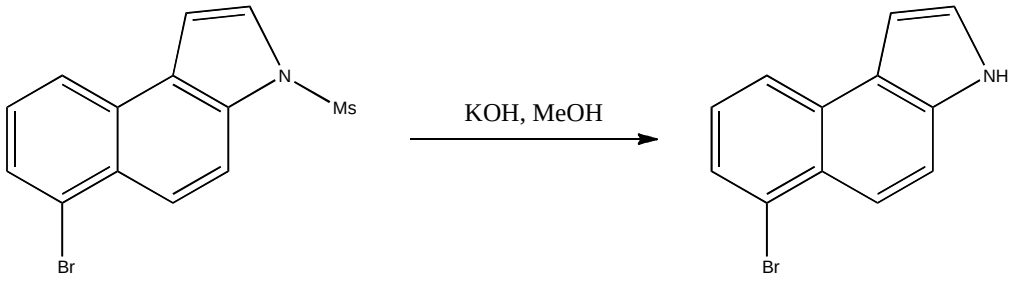

6-bromo-3-(methylsulfonyl)-3*H*-benzo[*e*]indole

5

6-bromo-3*H*-benzo[*e*]indole

6

Scheme 6

Compound 6 was produced with 28% yield using this saponification reaction (*Scheme 6*). This compound was the first purified product since **Compound 3**. This step has the lowest yield of any in the synthesis. It is unclear whether this loss of yield occurs during the reaction itself or during the purification process. The reaction occurs in methanol at reflux and was purified by high vacuum sublimation. It should be noted that different reflux durations have lead to vastly different yields with the most effective being between 12-24 hours.

The identity of **Compound 6** was confirmed by ^{1}H and ^{13}C NMR. The primary indicator that compound **6** was successfully made is the removal of the mesylate peak around 3 ppm. The indole peaks were observed at 7.31 ppm and 7.08 ppm are still present in compound **6** as well as the appropriate aromatic peaks (7-8 ppm). The indole peaks appeared as singlet peaks on the NMR of compound **6**. The expected 12 carbon peaks were observed in the ^{13}C NMR .

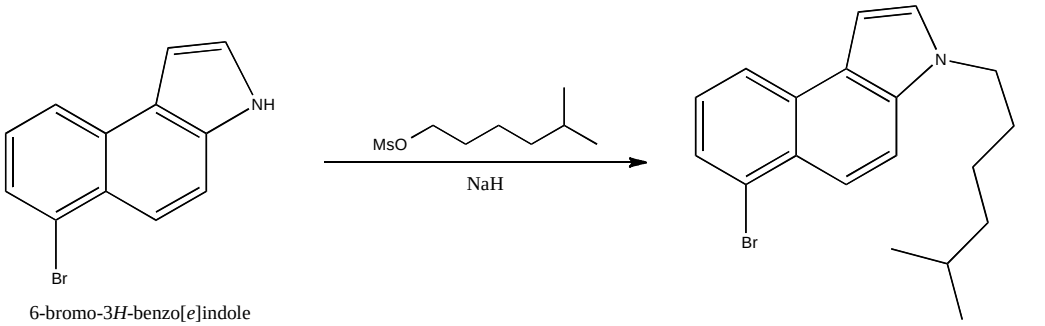

6-bromo-3*H*-benzo[*e*]indole

6

6-bromo-3-(5-methylhexyl)-3*H*-benzo[*e*]indole

7

Scheme 7

Compound 7 was produced with 95% yield (*Scheme 7*). The attachment of the alkyl chain proceeds using an S_N2 mechanism. The reaction was monitored by TLC using 4% EtOAC/ 96% hexanes. Additional additions of alkyl chain as well as additional NaH had to be added to drive the reaction to completion. Generally, two of three additions of NaH and alkyl chain were required. Initially, this reaction would not proceed due to excess mesthanesulfonyl choloride present in the alkyl chain. This was solved by purification by distillation of the alkyl chain.

The identity of **Compound 7** was confirmed by ^{1}H and ^{13}C NMR. The indole peak was observed at 7.21 ppm (J=2.38 Hz) and at 7.03 (J=2.67 Hz). The alkyl peaks appeared between 1-2 ppm with one appearing at 4.2 ppm, downshifted due to the neighboring nitrogen. The expected 18 carbon peaks were observed in the ^{13}C NMR.

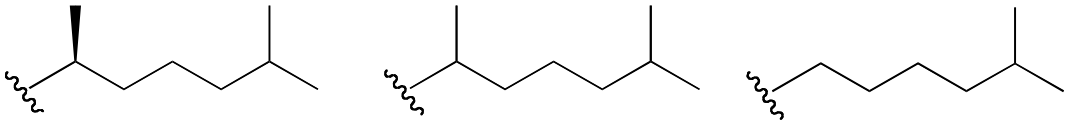

S chiral center Racemic No chiral center

Figure 10

Initially, the alkyl chain was to have the *S* chiral center configuration as depicted in *Figure 10*. Unfortunately, this stereoisomer was unable to be isolated or synthesized. Instead of using the racemic mixture of both stereoisomers the chiral center was removed all together. In **Compound 7** the alkyl chain has no chiral center.

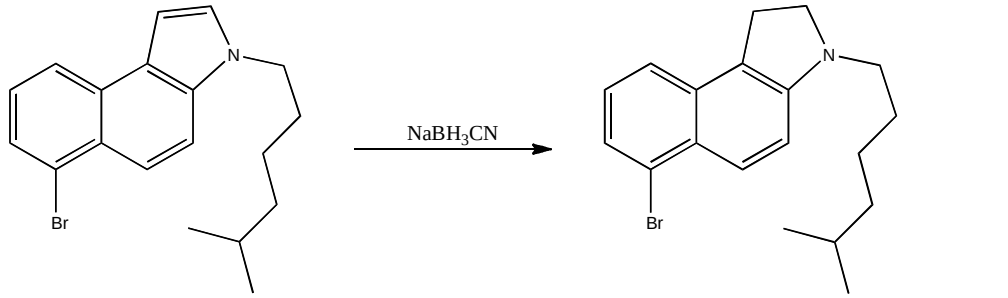

6-bromo-3-(5-methylhexyl)-3*H*-benzo[*e*]indole **7**

6-bromo-3-(5-methylhexyl)-2,3-dihydro-1*H*-benzo[*e*]indole **8**

Scheme 8

Compound 8 was produced in 86% yield (*Scheme 8*). This reduction was performed over two days. Two additional portions of $NaBH_3CN$ were added to ensure completion of the reaction. Initially, attempts to purify compound **8** with high vacuum sublimation failed as the product began to distill off the sublimation tip. So a high vacuum distillation was preformed as a means of purification.

The identity of **Compound 8** was confirmed by ^{1}H NMR and ^{13}C NMR. The disappearance of the indole peaks, the appearance of alkane peaks between 3-

4 ppm confirmed the reaction in *Scheme 8* was successful. The expected 18 carbon peaks were observed.

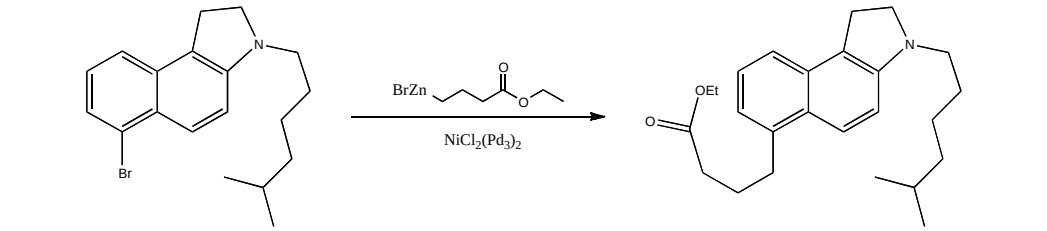

6-bromo-3-(5-methylhexyl)-2,3-dihydro-1*H*-benzo[*e*]indole

8

ethyl 4-(3-(5-methylhexyl)-2,3-dihydro-1*H*-benzo[*e*]indol-6-yl)butanoate

9

Scheme 9

Compound 9 was reported in over 100% yield (*Scheme 9*). It was synthesized using a Negishi coupling mechanism with $NiCl_2(Pd_2)_3$ as the catalyst. Initially, the reaction would not proceed on other model molecules, but this was solved once the DMAC was purified by distillation. This reaction was monitored by TLC using 4% EtOAc/ 96% hexanes as the mobile phase. Additional $NiCl_2(Pd_2)_3$ and ethoxy-4-oxobutylzinc bromide was added until the reactant spot disappeared on the TLC.

The identity of **Compound 9** was confirmed by ^{1}H NMR. The most telling sign is the presence of a quartet around 4 ppm which indicates the presence of the α-carbon to the ester. Although the ^{1}H NMR showed all the proper peaks it also showed low levels of impurities in the sample. The ^{13}C NMR sample was too crude to provide evidence of **9**.

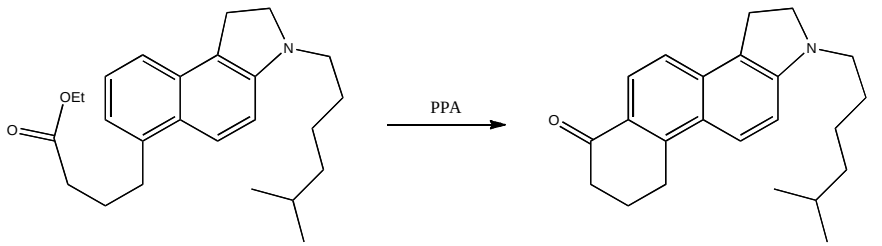

ethyl 4-(3-(5-methylhexyl)-2,3-dihydro-1*H*-benzo[*e*]indol-6-yl)butanoate **9**

1-(5-methylhexyl)-2,3,8,9-tetrahydro-1*H*-naphtho[2,1-*e*]indol-6(7*H*)-one **10**

Scheme 10

Compound 10 was produced in 36% yield. PPA acts as a Lewis acid for this ring closure (*Scheme 10*). These final two steps were only performed once and further trials, in order to learn reactant and catalyst amounts as well as reaction duration, are needed to maximize the yields of these reactions. Compound **10** was purified by high vacuum sublimation.

The identity of **Compound 10** was confirmed by ^{1}H NMR. Another sign that product is obtained is that in solution under UV light, compound **10** fluoresces a blue-green color as the PRODAN molecule is now successfully imbedded into the model. In total, from reactant compound **1** to product compound **10** a total percent yield of 10.2% was obtained.

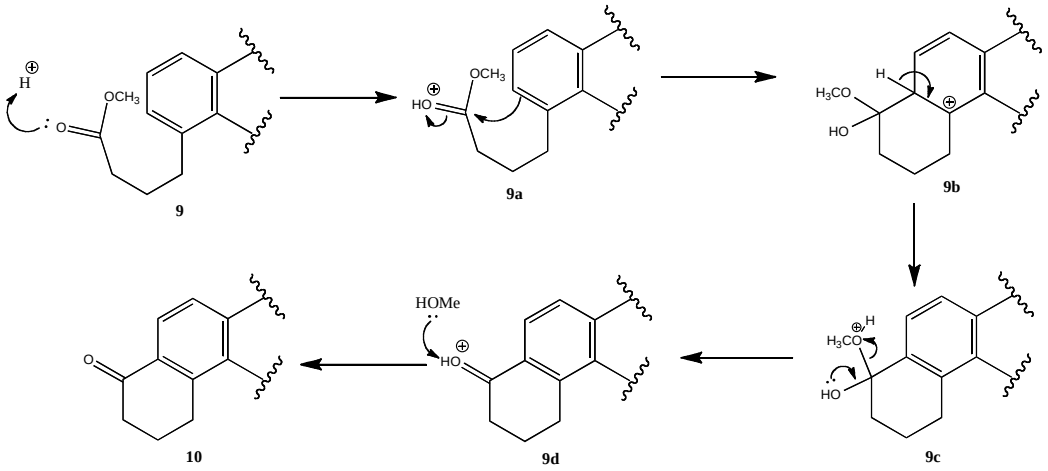

Figure 11

The mechanism for the A-ring closure is worth nothing (*Figure 11*). This mechanism functions in a similar manner to that of the ring closure on the D-ring. A hydrogen from the Lewis acid PPA is attacked nucleophillically by a lone pair on the ester carbonyl group in **9**. The carbonyl carbon is then attacked by pi electrons in the aromatic ring, creating a carbon-carbon bond sealing the 6-membered ring in **9a**. Aromaticity is restored in **9b**. In a manner similar to a reverse aldol reaction the lone pair on the alcohol reforms a carbonyl and the OCH_3^+ acts as a leaving group in **9c**. Finally, the hydrogen is removed from the carbonyl in **9d** and the final product **Compound 10** is obtained.

Conclusion

The starting compound 1-(5-methylhexyl)-2,3,8,9-tetrahydro-1*H*-naphtho[2,1-*e*]indol-6(7*H*)-one was prepared with a 10.2% yield from starting 5-Bromonaphthalen-2-ol. The final product needs to be analyzed and characterized by fluorescence spectroscopy. Also, *Scheme 6*, *Scheme 9*, and *Scheme 10* all need further examination. These three steps all resulted in the lowest yields, and drastically reduce the yield of the synthesis. The reaction time in *Scheme 6* needs further examination in order to determine the proper amount of reflux and appropriate temperature. *Scheme 9* and *Scheme 10* were only performed once and further exploration of these reactions is necessary to maximize the yield. The proper duration of the reactions, the amount of reactants used, and the best possible purification technique all need to be examined. Once these issues have been addressed the model can be used to examine cholesterol binding in HSA.

Appendix A

^{1}H and ^{13}C NMR Spectra

Figure A1. 5-Bromonaphthalen-2-amine ^{1}H-NMR 4.13 6.83

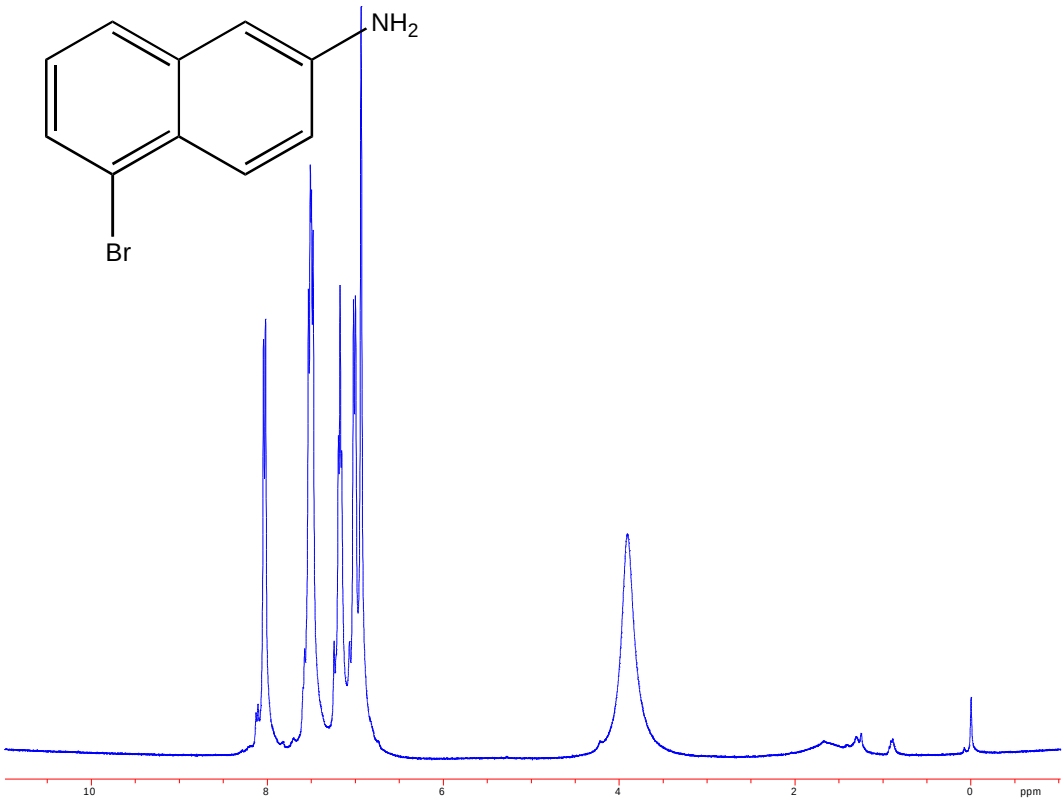

Figure A2. 5-Bromonaphthalen-2-amine ^{13}C-NMR

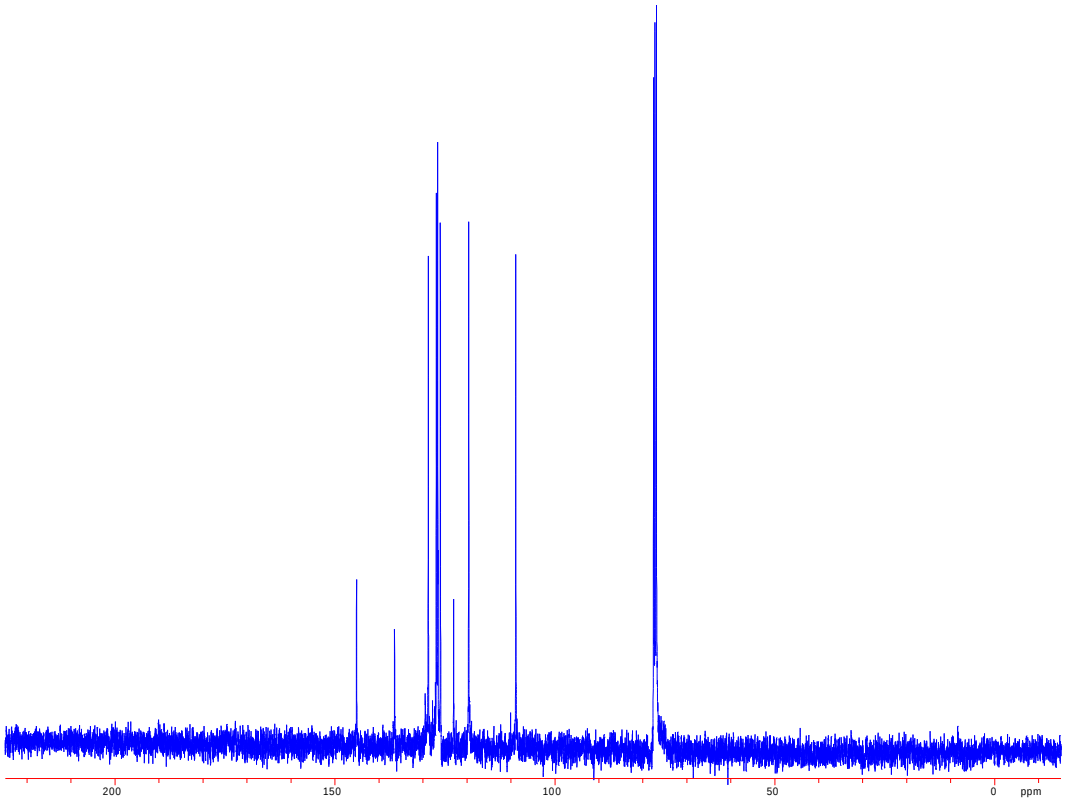

Figure A3. *N*-(5-Bromonaphthalen-2-yl)methanesulfonamide ^{1}H-NMR

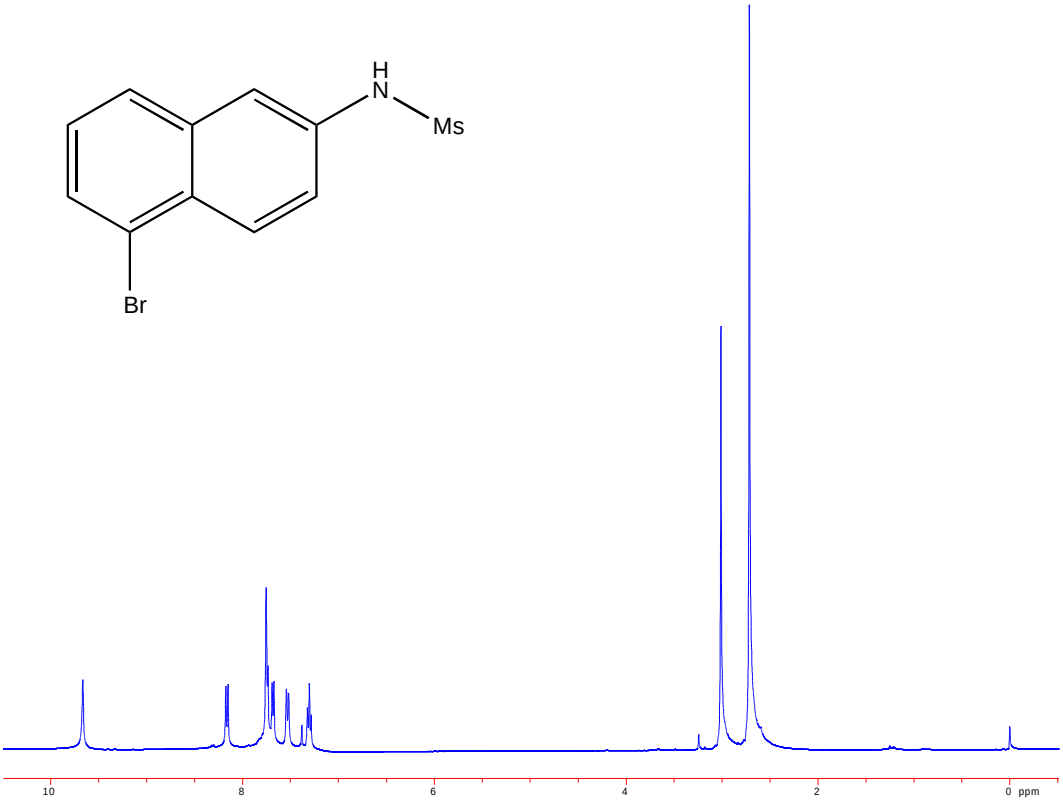

Figure A4. *N*-(5-Bromonaphthalen-2-yl)methanesulfonamide ^{13}C-NMR

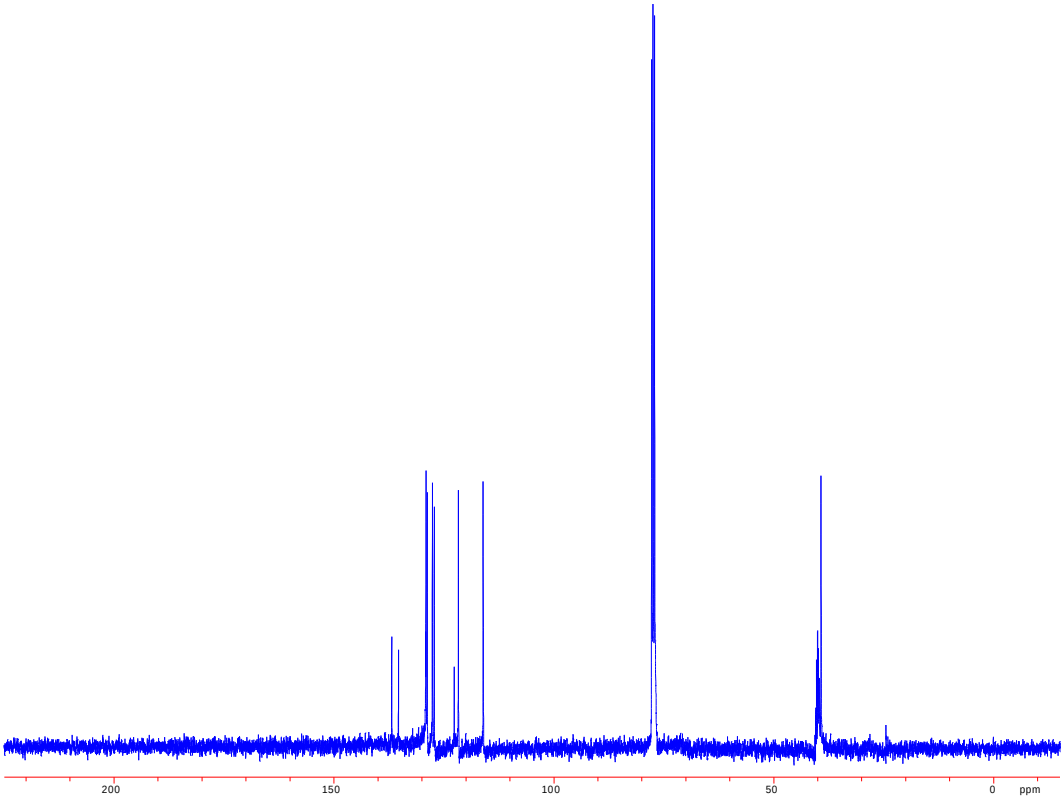

Figure A5. *N*-(5-Bromonaphthalen-2-yl)-*N*-(2,2-diethoxyethyl)methanesulfonamide ^{1}H-NMR

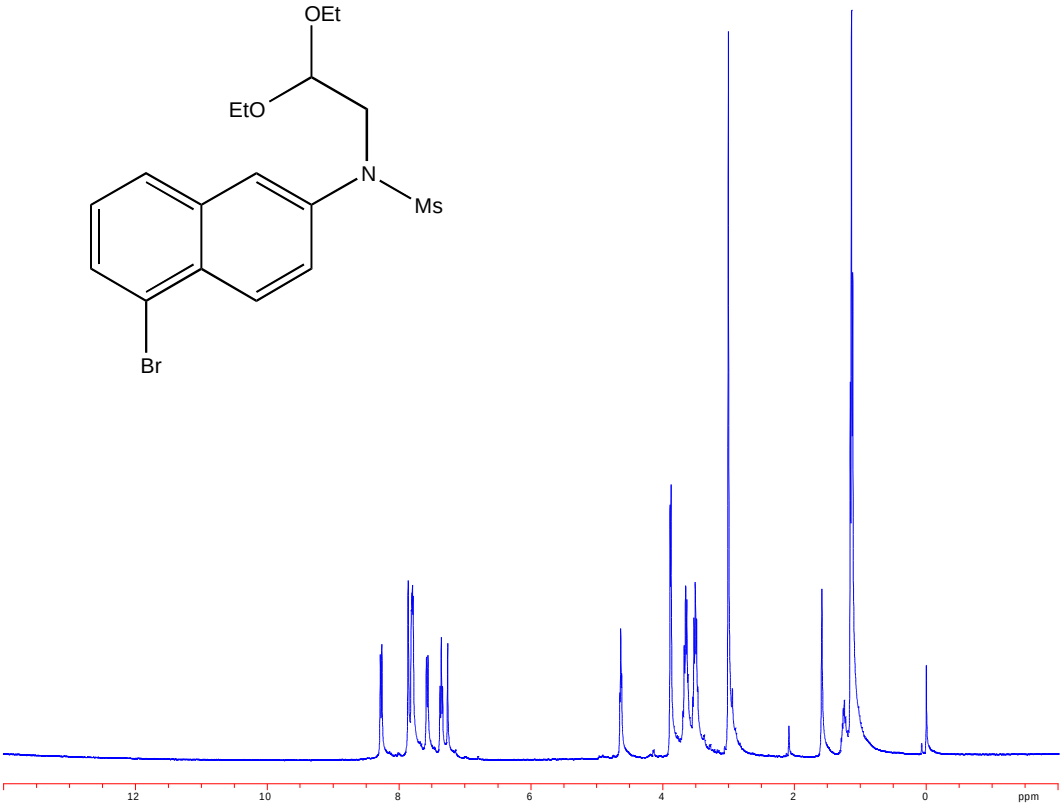

Figure A6. *N*-(5-Bromonaphthalen-2-yl)-*N*-(2,2-diethoxyethyl)methanesulfonamide ^{13}C-NMR

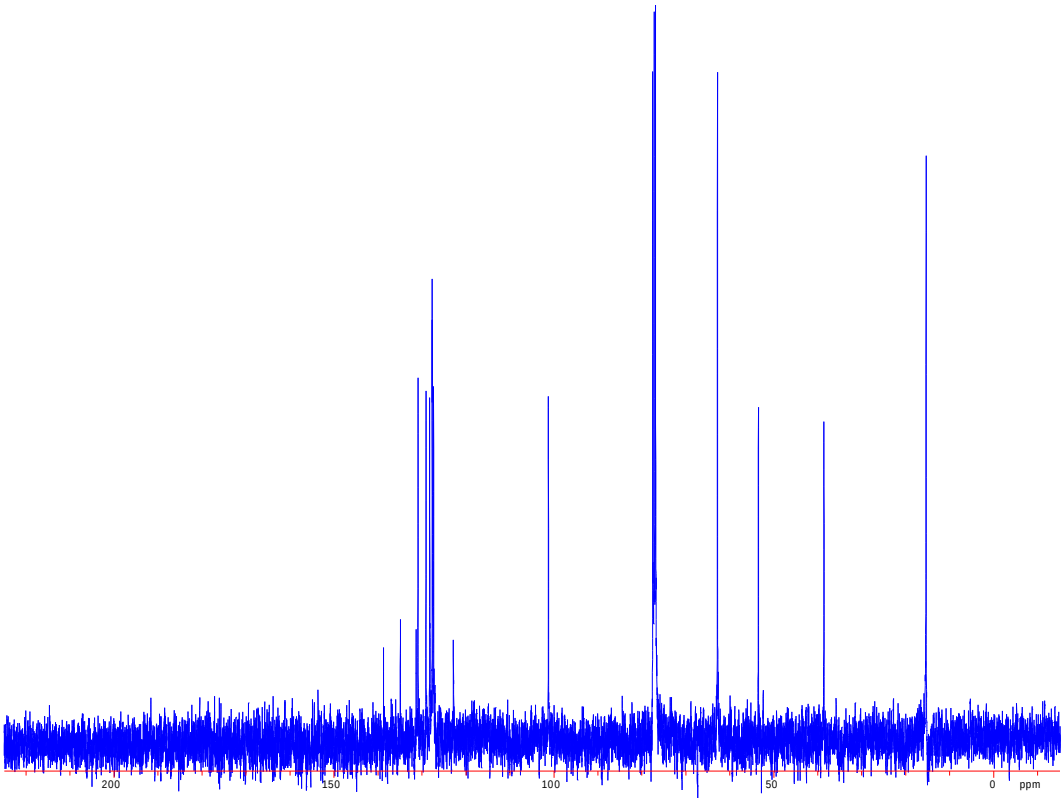

Figure A7. 6-Bromo-3-(methylsulfonyl)-3*H*-benzo[*e*]indole ^{1}H-NMR

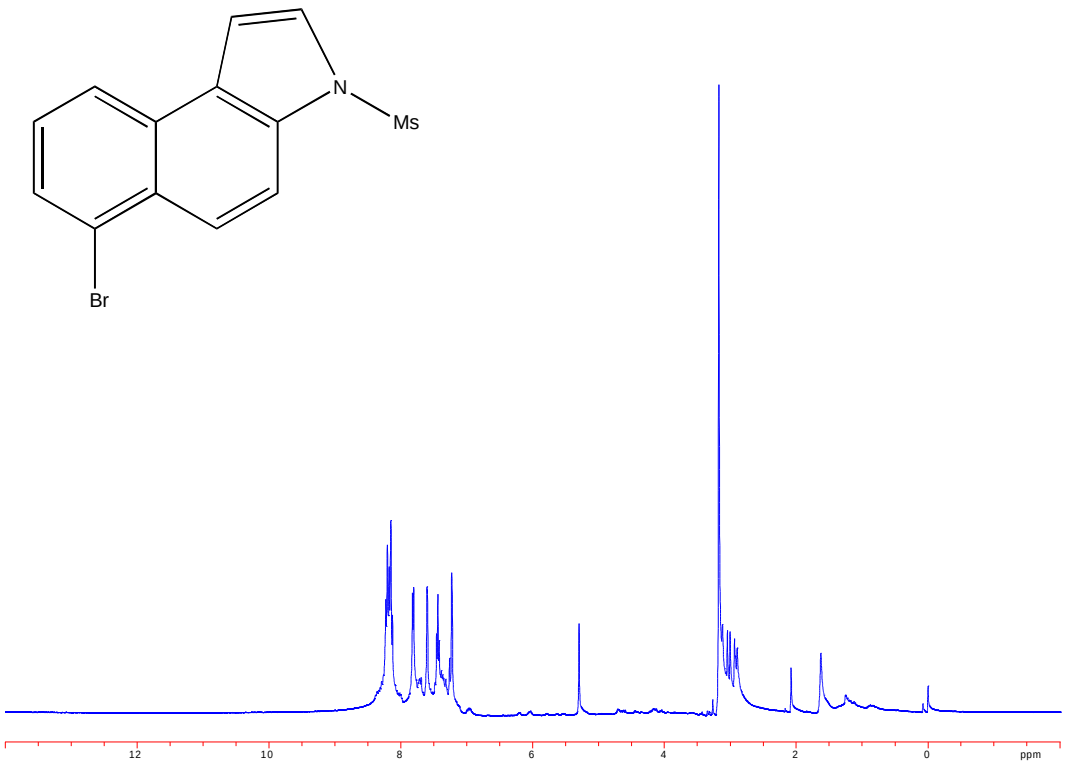

Figure A8. 6-Bromo-3-(methylsulfonyl)-3*H*-benzo[*e*]indole ^{13}C-NMR

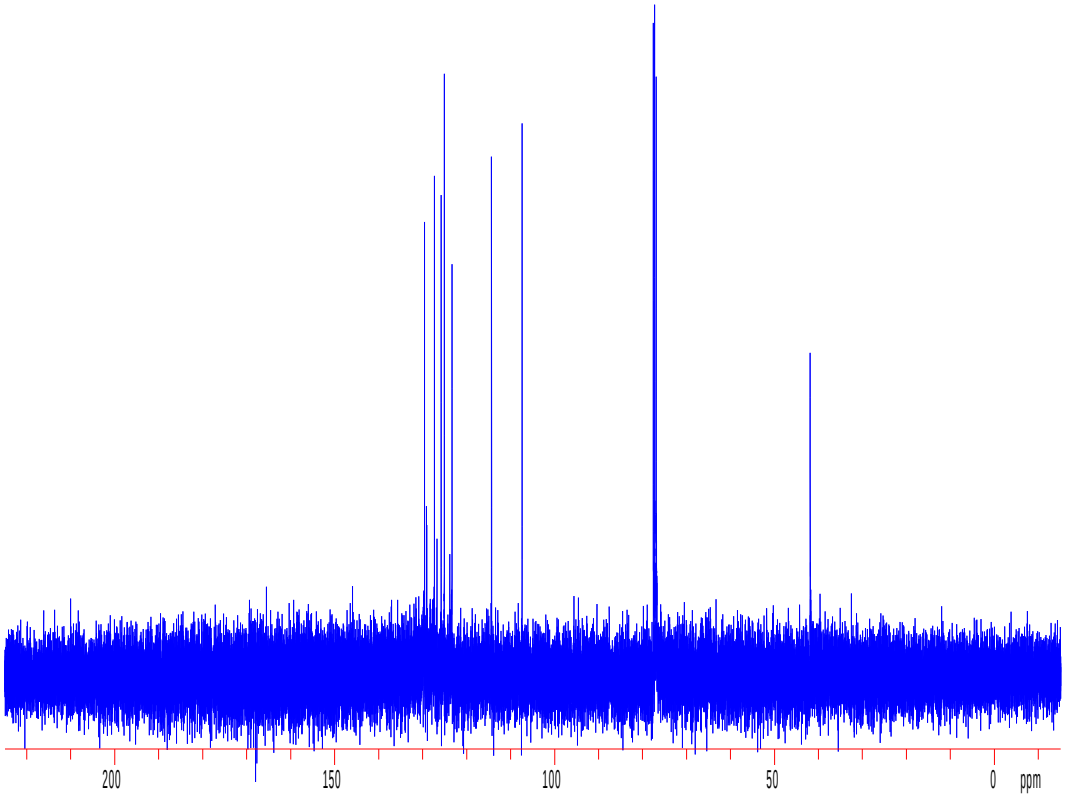

Figure A9. 6-Bromo-3*H*-benzo[*e*]indole ^{1}H-NMR

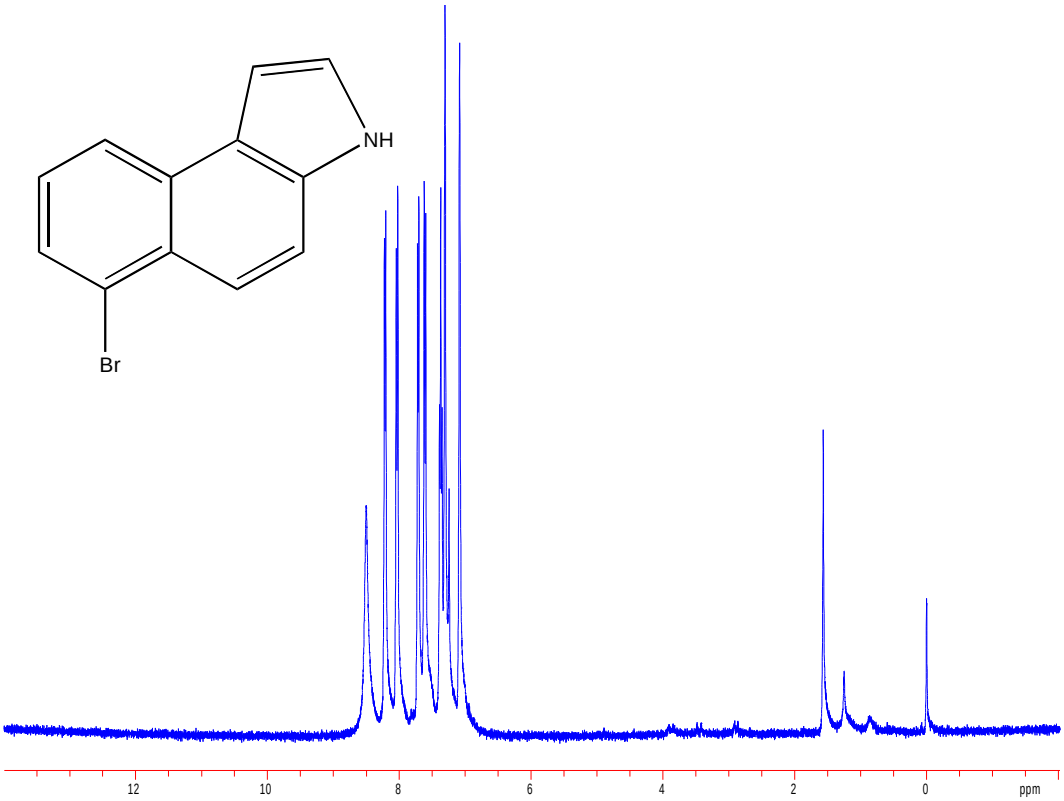

Figure A10. 6-Bromo-3*H*-benzo[*e*]indole ^{13}C-NMR

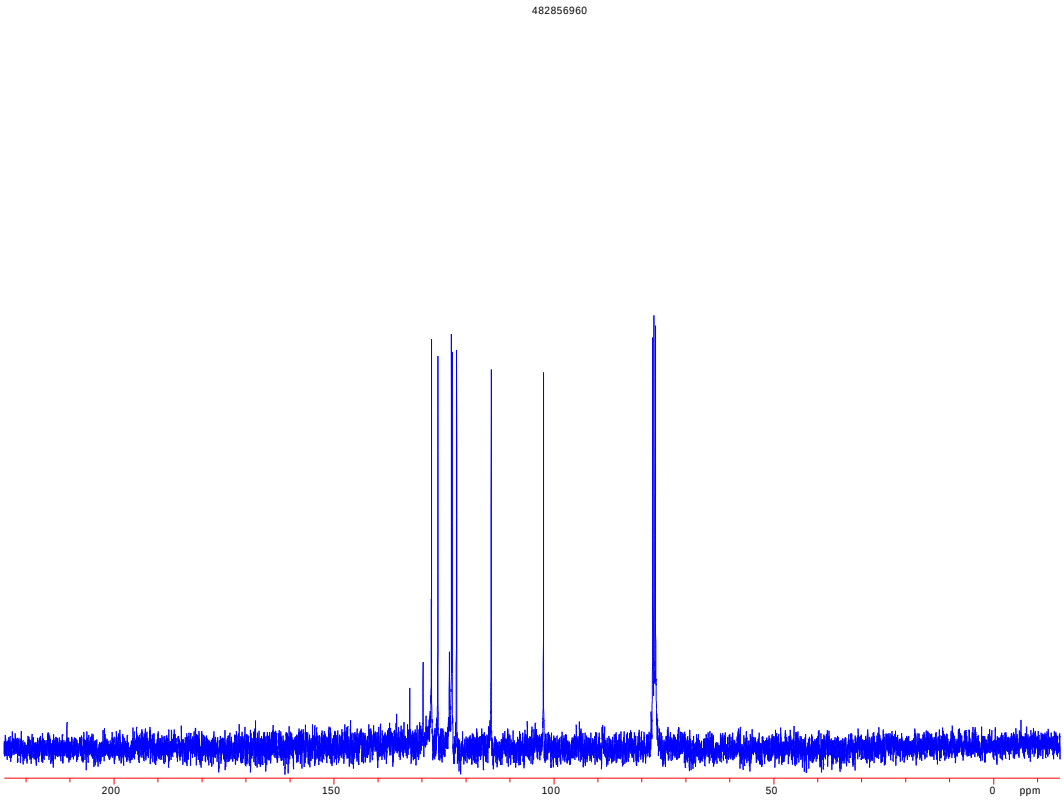

Figure A11. 6-bromo-3-(5-methylhexyl)-3*H*-benzo[*e*]indole. ^{1}H-NMR.

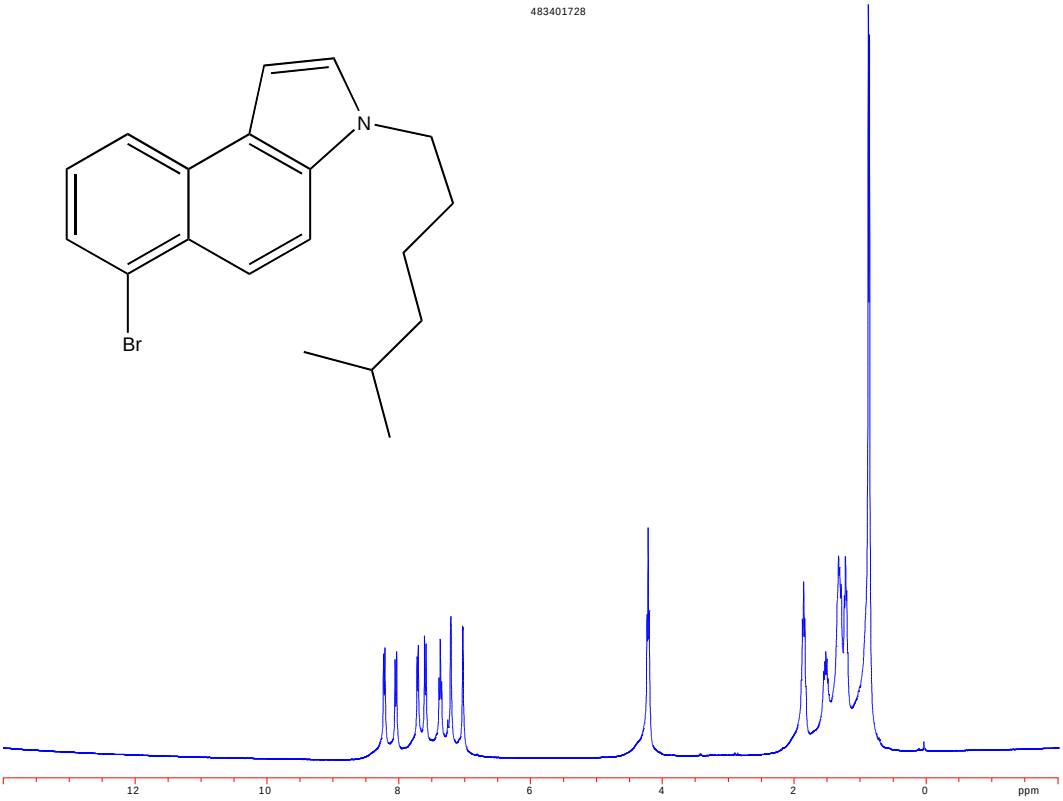

Figure A12. 6-bromo-3-(5-methylhexyl)-3*H*-benzo[*e*]indole. ^{13}C-NMR.

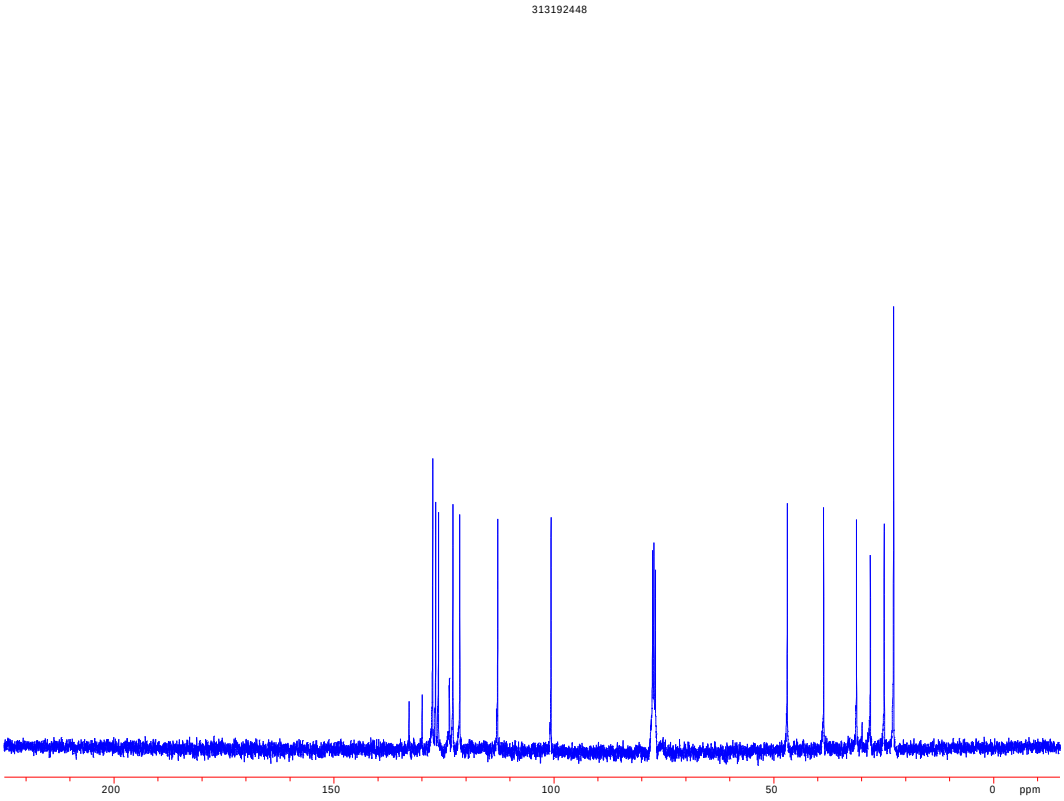

Figure A13. 6-Bromo-3-(5-methylhexyl)-2,3-dihydro-1*H*-benzo[*e*]indole ^{1}H-NMR.

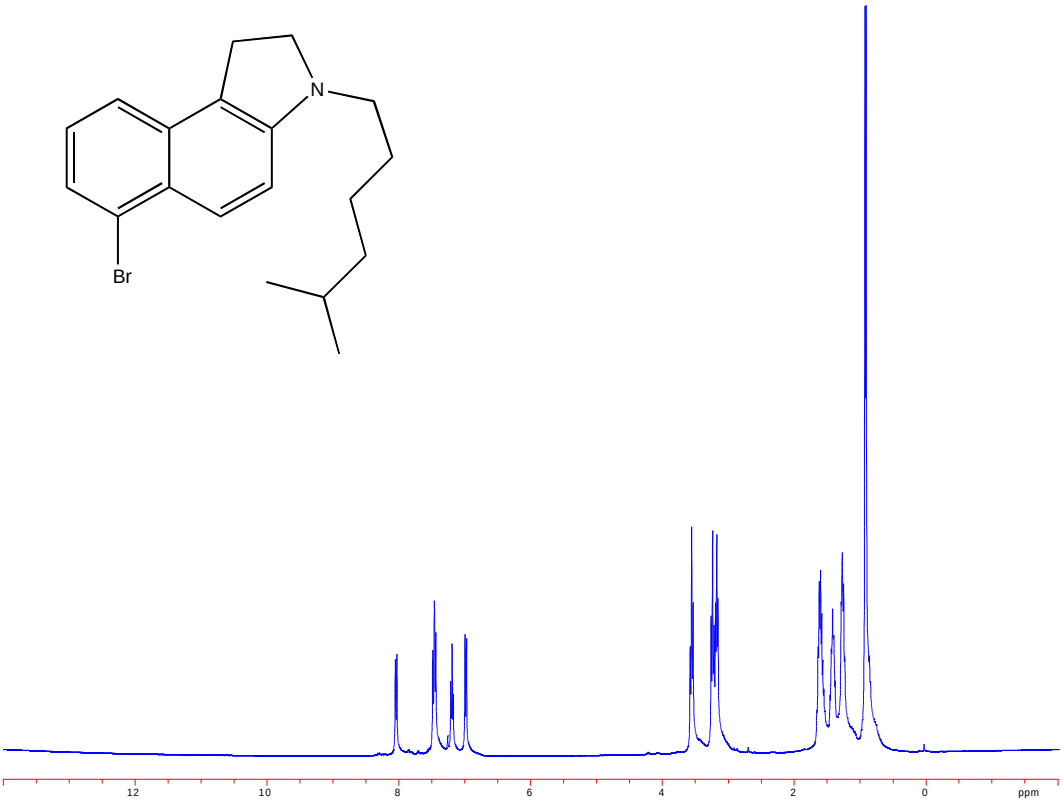

Figure A14. 6-Bromo-3-(5-methylhexyl)-2,3-dihydro-1*H*-benzo[*e*]indole ^{13}C-NMR.

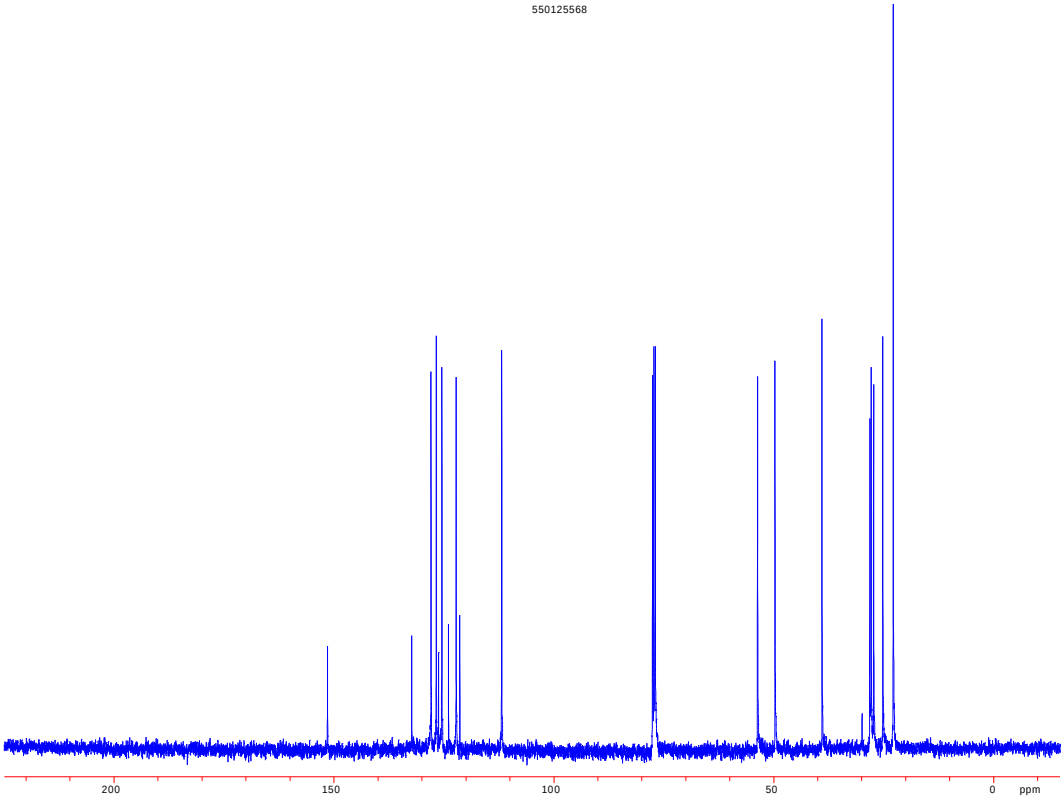

Figure A15. Ethyl 4-(3-(5-methylhexyl)-2,3-dihydro-1*H*-benzo[*e*]indol-6-yl)butanoate ^{1}H-NMR.

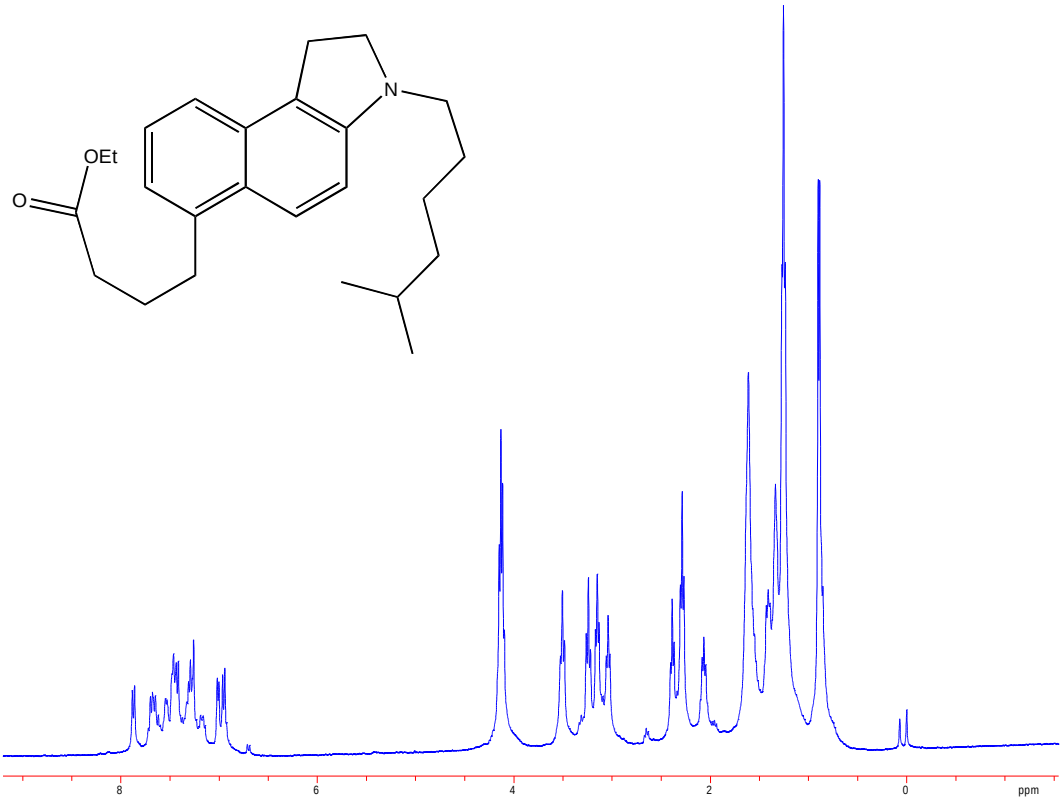

Figure A16. Ethyl 4-(3-(5-methylhexyl)-2,3-dihydro-1*H*-benzo[*e*]indol-6-yl)butanoate ^{13}C-NMR. (Crude)

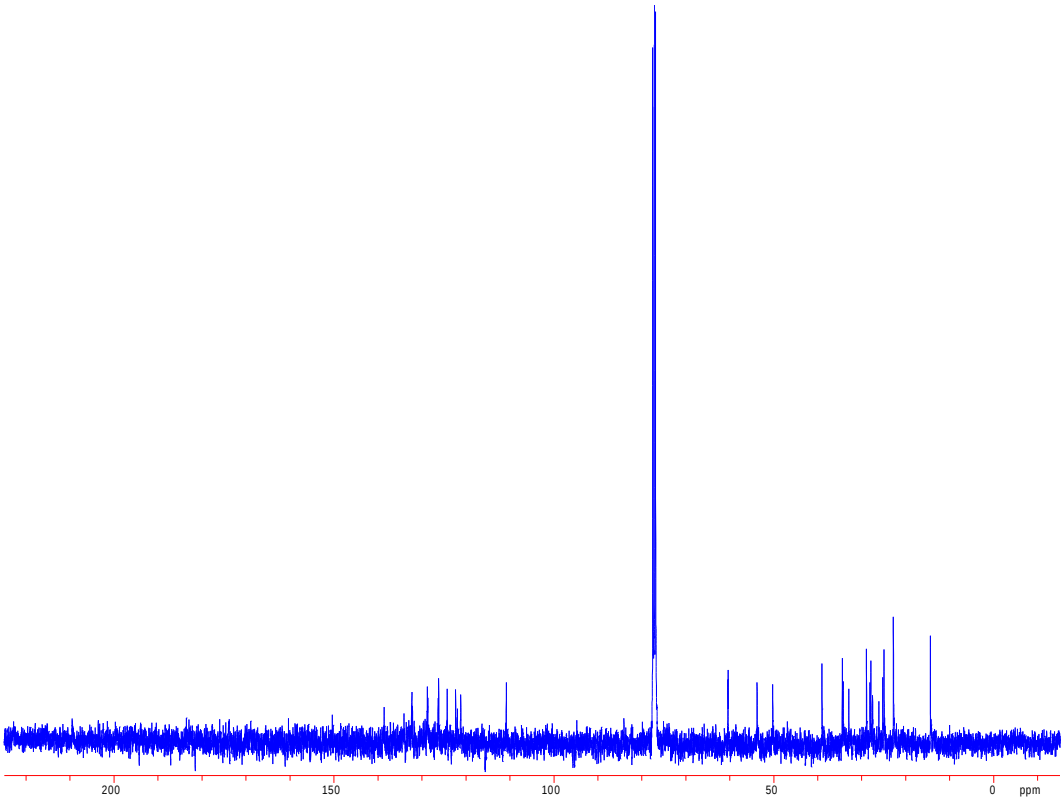

Figure A17. 1-(5-methylhexyl)-2,3,8,9-tetrahydro-1*H*-naphtho[2,1-*e*]indol-6(7*H*)-one ^{1}H-NMR.

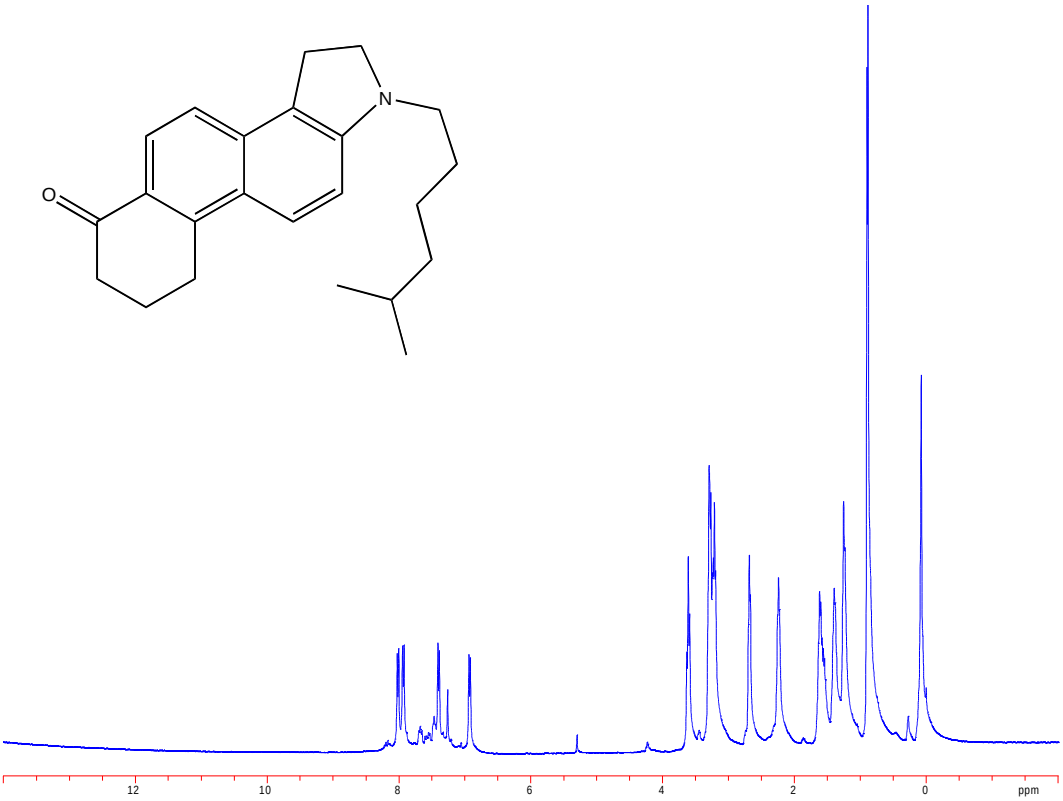

Figure A18. 1-(5-methylhexyl)-2,3,8,9-tetrahydro-1*H*-naphtho[2,1-*e*]indol-6(7*H*)-one ^{13}C-NMR. (Crude)

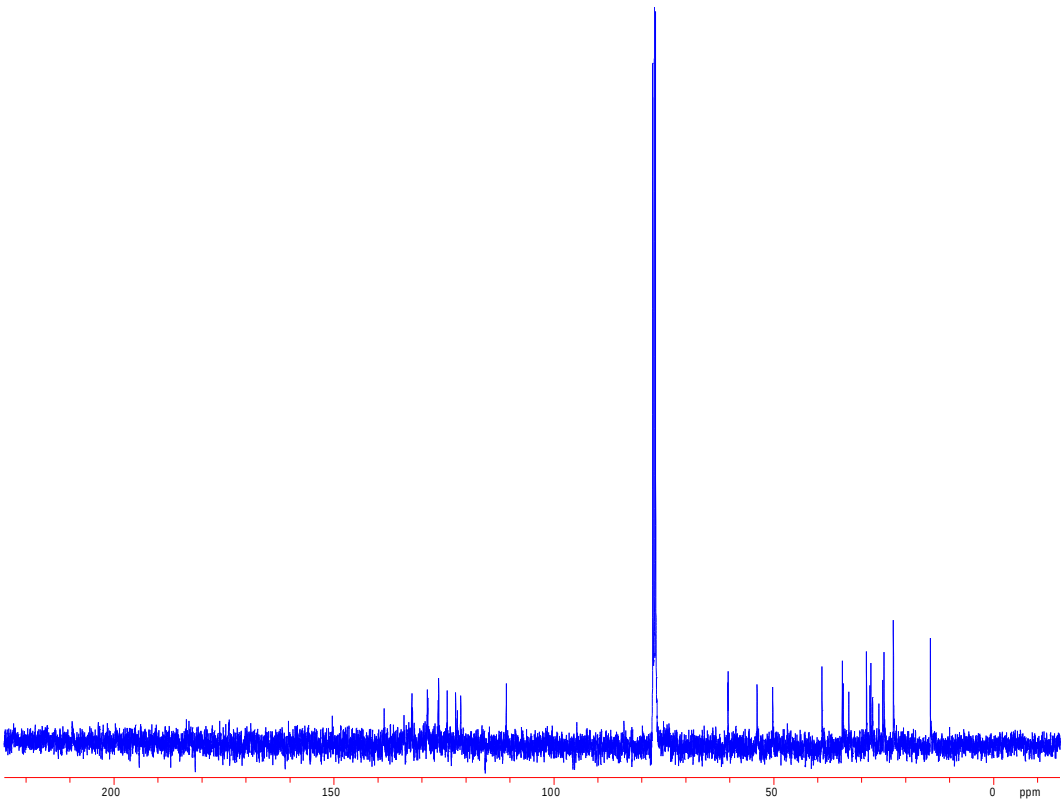

References

[i] Zhao, Y., & Marcel, Y. L. (1996). Serum albumin is a significant intermediate in cholesterol transfer between cells and lipoproteins†. *Biochemistry, 35*(22), 7174-7180.

[ii] McKee, T.; McKee, J. R. Biochemistry The Molecular Basis of Life; Oxford University Press, New York, NY, 2009. 386-394.

[iii] Barter, P., & Rye, K. A. (1996). High density lipoproteins and coronary heart disease. *Atherosclerosis, 121*(1), 1-12.

[iv] Zhao, Y., & Marcel, Y. L. (1996). Serum albumin is a significant intermediate in cholesterol transfer between cells and lipoproteins†. *Biochemistry, 35*(22), 7174-7180.

[v] Sugio, S., Kashima, A., Mochizuki, S., Noda, M., & Kobayashi, K. (1999). Crystal structure of human serum albumin at 2.5 Å resolution. *Protein Engineering, 12*(6), 439.

[vi] Ha, J. S., Ha, C. E., Chao, J. T., Petersen, C. E., Theriault, A., & Bhagavan, N. V. (2003). Human serum albumin and its structural variants mediate cholesterol efflux from cultured endothelial cells. *Biochimica Et Biophysica Acta (BBA)-Molecular Cell Research, 1640*(2-3), 119-128.

[vii] Ghuman, J., Zunszain, P. A., Petitpas, I., Bhattacharya, A. A., Otagiri, M., & Curry, S. (2005). Structural basis of the drug-binding specificity of human serum albumin. *Journal of Molecular Biology, 353*(1), 38-52.

[viii] Carter, D. C., He, X. M., Munson, S. H., Twigg, P. D., Gernert, K. M., Broom, M. B., et al. (1989). Three-dimensional structure of human serum albumin. *Science, 244*(4909), 1195.

[ix] Bhattacharya, A. A., Grüne, T., & Curry, S. (2000). Crystallographic analysis reveals common modes of binding of medium and long-chain fatty acids to human serum albumin1. *Journal of Molecular Biology, 303*(5), 721-732.

[x] Kuller, L. H., Eichner, J. E., Orchard, T. J., Grandits, G. A., McCallum, L., & Tracy, R. P. (1991). The relation between serum albumin levels and risk of coronary heart disease in the multiple risk factor intervention trial. *American Journal of Epidemiology, 134*(11), 1266.

[xi] Goldwasser, P., & Feldman, J. (1997). Association of serum albumin and mortality risk. *Journal of Clinical Epidemiology, 50*(6), 693-703.

[xii] Ha, J. S., Ha, C. E., Chao, J. T., Petersen, C. E., Theriault, A., & Bhagavan, N. V. (2003). Human serum albumin and its structural variants mediate cholesterol efflux from cultured endothelial cells. *Biochimica Et Biophysica Acta (BBA)-Molecular Cell Research, 1640*(2-3), 119-128.

[xiii] Frostell-Karlsson, A., Remaeus, A., Roos, H., Andersson, K., Borg, P., Hamalainen, M., et al. (2000). Biosensor analysis of the interaction between immobilized human serum albumin and drug compounds for prediction of human serum albumin binding levels. *J.Med.Chem, 43*(10), 1986-1992.

[xiv] Ghuman, J., Zunszain, P. A., Petitpas, I., Bhattacharya, A. A., Otagiri, M., & Curry, S. (2005). Structural basis of the drug-binding specificity of human serum albumin. *Journal of Molecular Biology*, *353*(1), 38-52.

[xv] Gimpl, G., & Gehrig-Burger, K. (2007). Cholesterol reporter molecules. *Bioscience Reports, 27*(6), 335-358.

[xvi] Mukherjee, S., Zha, X., Tabas, I., & Maxfield, F. R. (1998). Cholesterol distribution in living cells: Fluorescence imaging using dehydroergosterol as a fluorescent cholesterol analog. *Biophysical Journal, 75*(4), 1915-1925.

[xvii] Gimpl, G., & Gehrig-Burger, K. (2007). Cholesterol reporter molecules. *Bioscience Reports, 27*(6), 335-358.

[xviii] Scheidt, H. A., Müller, P., Herrmann, A., & Huster, D. (2003). The potential of fluorescent and spin-labeled steroid analogs to mimic natural cholesterol. *Journal of Biological Chemistry, 278*(46), 45563.

[xix] Moreno, F., Cortijo, M., & González - Jiménez, J. (1999). The fluorescent probe prodan characterizes the warfarin binding site on human serum albumin. *Photochemistry and Photobiology, 69*(1), 8-15.

[xx] Krishnakumar, S. S., & Panda, D. (2002). Spatial relationship between the prodan site, trp-214, and cys-34 residues in human serum albumin and loss of structure through incremental unfolding†. *Biochemistry*, *41*(23), 7443-7452.

[xxi] Weber, G., & Farris, F. J. (1979). Synthesis and spectral properties of a hydrophobic fluorescent probe: 6-propionyl-2-(dimethylamino) naphthalene. *Biochemistry*, *18*(14), 3075-3078.

[xxii] Lobo, B. C., & Abelt, C. J. (2003). Does PRODAN possess a planar or twisted charge-transfer excited state? photophysical properties of two PRODAN derivatives. *J.Phys.Chem.A*, *107*(50), 10938-10943.

[xxiii] Davis, B. N., & Abelt, C. J. (2005). Synthesis and photophysical properties of models for twisted PRODAN and dimethylaminonaphthonitrile. *J.Phys.Chem.A*, *109*(7), 1295-1298.

Vita

Nicholas Adam Lopez

Nicholas Adam Lopez was born in San Jose, California on November 18, 1989. He graduated from Potomac Falls High School in Sterling, VA in June 2007. Then he went on to attend the College of William and Mary in Williamsburg, VA and will receive a Bachelors of Science in Chemistry in May 2011.